ACS SENSORS

pubs.acs.org/acssensors
Review

Paper-Based Vertical Flow Assays for in Vitro Diagnostics and Environmental Monitoring

Jaehyung Jeon, Heeseon Choi, Gyeo-Re Han, Rajesh Ghosh, Barath Palanisamy, Dino Di Carlo, Aydogan Ozcan,* and Sungsu Park*

Cite This: *ACS Sens.* 2025, 10, 3317−3339
Read Online
ACCESS | Metrics & More | Article Recommendations

ABSTRACT: Microfluidic paper-based analytical devices (μPADs) are powerful tools for diagnostic and environmental monitoring. Being affordable and portable, μPADs enable rapid detection of small molecules, heavy metals, and biomolecules, thereby decentralizing diagnostics and expanding biosensor accessibility. However, the reliance on two-dimensional fluid flow restricts the utility of conventional μPADs, presenting challenges for applications that require simultaneous multibiomarker analysis from a single sample. Vertical flow paper-based analytical devices (VF-μPADs) overcome this challenge by allowing axial fluid movement through paper stacks, offering several advantages, including (1) enhanced multiplexing capabilities, (2) reduced hook effect for improved accuracy, and (3) shorter assay times. This review provides an overview of VF-μPADs technologies, exploring structural and functional performance trade-offs between VF-μPADs and conventional lateral flow systems. The sensing performance, fabrication methods, and applications in in vitro diagnostics and environmental monitoring are discussed. Furthermore, critical challenges—such as fabrication complexity, data analysis, and scalability—are addressed, along with proposed strategies for mitigating these barriers to facilitate broader adoption. By examining these strengths and challenges, this review presents the potential of VF-μPADs to advance point-of-care testing, particularly in resource-limited settings.

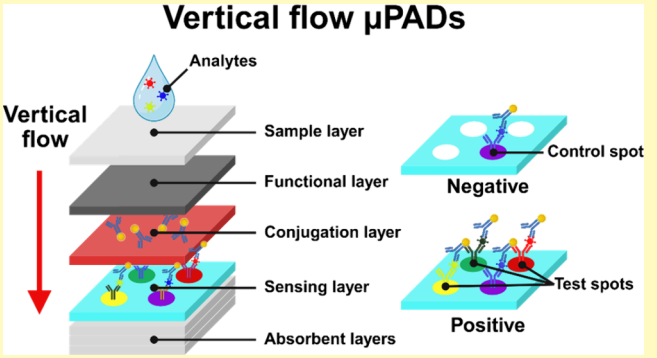

KEYWORDS: *Paper-based analytical devices, Vertical flow paper-based analytical devices, Vertical flow assay, In vitro diagnostics, Environmental monitoring, Multiplexing, Point of care testing*

The use of paper as a medium for analytical testing dates back to the early 20th century. However, paper began to be systematically used for diagnostic purposes only in the latter half of the century. Lateral flow assays (LFAs), also known as immunochromatographic assays, are among the earliest and most widely adopted paper-based analytical devices (PADs). Exploiting the capillary action of paper to transport samples and reagents, these assays facilitate rapid and user-friendly diagnostic testing.[1−4] One key advantage of LFAs is their simplified and scalable manufacturing process. Multiple components, such as sample pads, conjugation pads, nitrocellulose (NC) membranes, and absorbent pads, are assembled within a single frame and then processed into individual test strips through a precise cutting mechanism. This approach streamlines production while overcoming material complexity, making LFAs highly cost-effective for large-scale manufacturing. While LFAs have proven remarkably successful due to their simplified assay procedures, particularly for applications such as pregnancy testing and infectious disease screening, they are inherently limited by their one-dimensional (1D) flow. This restriction hinders their ability to support multiplexed testing and sequential reactions within a single assay.

In 2007, the integration of microfluidics with paper-based platforms led to a significant advancement in the form of "microfluidic" PADs (μPADs). Pioneered by Whitesides and colleagues, μPADs utilized patterning technology to create hydrophobic barriers on paper, directing fluids through the remaining hydrophilic channels.[5,6] This approach enabled the design of diverse two-dimensional (2D) fluidic pathways, allowing for multistep assays while minimizing reagent consumption. However, μPADs still face challenges in multiplexing and reproducibility due to their reliance on complex fluidic pathways, where minor deviations in test

Received: February 26, 2025
Revised: April 22, 2025
Accepted: May 6, 2025
Published: May 15, 2025

https://doi.org/10.1021/acssensors.5c00668
ACS Sens. 2025, 10, 3317−3339

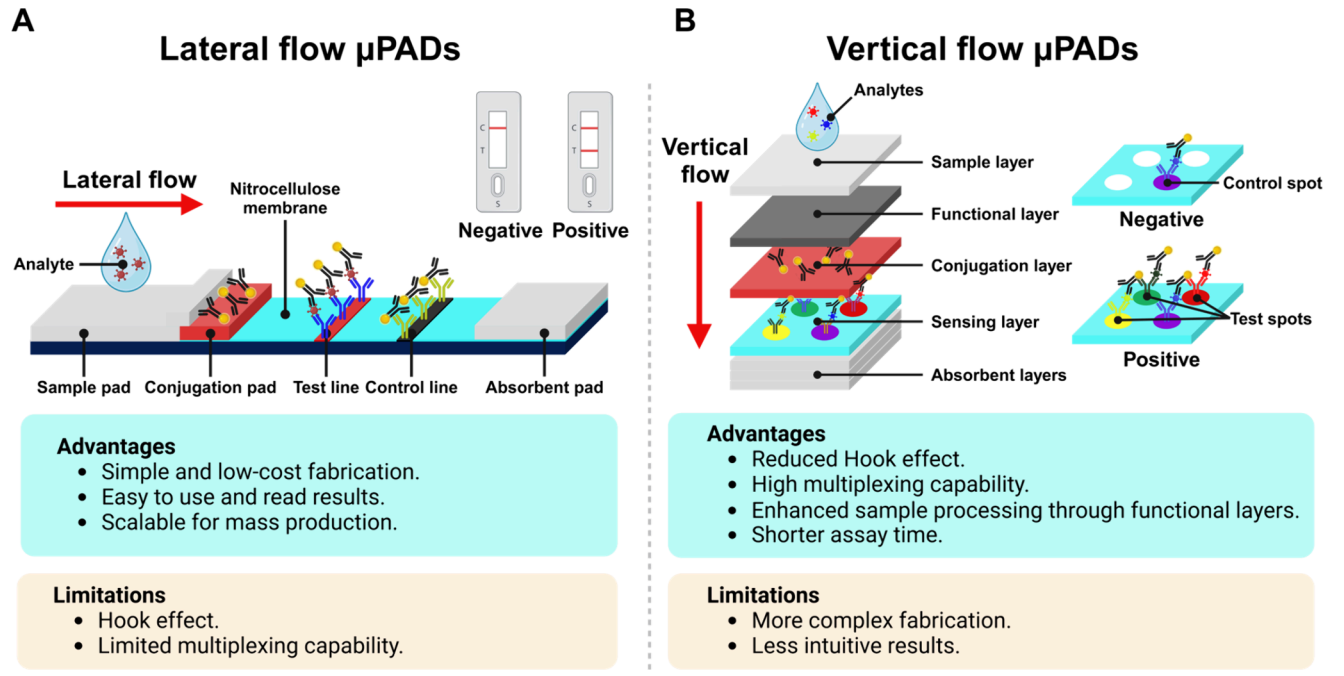

Figure 1. Comparison of lateral flow-μPADs (LF-μPADs) and VF-μPADs. (A) LF-μPADs leverage horizontal fluid flow across a porous membrane, making them simple, cost-effective, and scalable for mass production, with easily interpretable results. However, they are constrained by the hook effect at high analyte concentrations and offer limited multiplexing abilities. (B) VF-μPADs harness vertical fluid flow through stacked paper layers, enabling enhanced multiplexing capabilities, reduced hook effect, and the integration of functional layers to accommodate complex samples. Despite these advantages, VF-μPADs face challenges with more intricate fabrication and less intuitive result interpretation.

properties—such as permeability and ambient humidity—can be amplified across multiple assay steps, increasing overall variability. This can cause uneven flow distribution, line interference, and the hook effect[7,8]—a phenomenon where, at high analyte concentrations, the measured signal intensity is lower than expected, leading to reduced diagnostic accuracy.

These limitations of μPADs have led to the development of "vertical flow" PADs (VF-μPADs), a novel category of paper-based devices that utilize the z-dimension of stacked paper layers for fluid transport.[7,9,10] This innovation enables the creation of complex three-dimensional fluidic networks, overcoming many of the limitations associated with two-dimensional flow while providing enhanced multiplexing capabilities, improved reproducibility, and greater control over fluid distribution. Consequently, VF-μPADs significantly reduce assay durations and humidity-based variation, primarily due to their shorter, enclosed flow path, which is reduced to a few millimeters compared to the several centimeters in lateral flow-based μPADs.[11] Moreover, VF-μPADs incorporate multiple test regions that are spatially isolated in a single sensing layer. Thus, they can circumvent the interference in lateral flow assays, where the placement of test lines and cross-talk between reaction zones can disrupt signal intensity, particularly in sequentially positioned test lines or reaction areas.[12−14] VF-μPADs are fabricated through various techniques, such as stacking,[6,15] folding,[16,17] and three-dimensional (3D) printing,[18] all of which employ porous membranes to construct vertical flow architectures. This multilayered structure allows VF-μPADs to incorporate additional functional layers, enabling tasks such as sample separation,[18] fluid distribution,[12] detection, and signal amplification.[19] Furthermore, VF-μPADs enable quantitative analysis, allowing for comprehensive quantification when paired with portable imaging systems.[12,20−22] Recent advancements in AI-based quantification have further enhanced the accuracy and reliability of VF-μPADs, providing more detailed test information for multiple analytes from a single sample.[20,21,23−25] This positions VF-μPADs as a robust platform for modern diagnostic and sensor technologies, particularly in resource-limited settings.

This review provides a comprehensive examination of VF-μPADs, highlighting their advantages over conventional μPADs. We begin by exploring how VF-μPADs enable improved sensor performance with multiplexing, followed by an evaluation of the various fabrication methods. Next, we discuss the applications of VF-μPADs in point-of-care testing (POCT) and environmental monitoring, highlighting their versatility across various fields. Furthermore, this review identifies the current challenges associated with VF-μPADs, including fabrication complexity, data analysis, and scalability, which must be overcome to enable broader adoption in clinical and field settings.

COMPARISON OF LATERAL FLOW AND VERTICAL FLOW μPADs

Lateral flow-μPADs (LF-μPADs) and "dip-stick" sensors are critical tools in POCT, each providing distinct advantages and limitations depending on their specific application areas (Figure 1A). LF-μPADs utilize lateral fluid movement across a single plane of the membrane through capillary action to transport fluids. As this is achieved without external pumps or power, LF-μPADs are ideal for POCT. Their structural simplicity, well-established manufacturing processes, and cost-effectiveness make them ideal for rapid, low-cost diagnostics, such as pregnancy tests and infectious disease screening. This is exemplified by the widespread use of LFA-based self-testing during the COVID-19 pandemic.[26] These advantages notwithstanding, LF-μPADs have many limitations, including limited multiplexing ability and the hook effect. In

https://doi.org/10.1021/acssensors.5c00668
ACS Sens. 2025, 10, 3317−3339

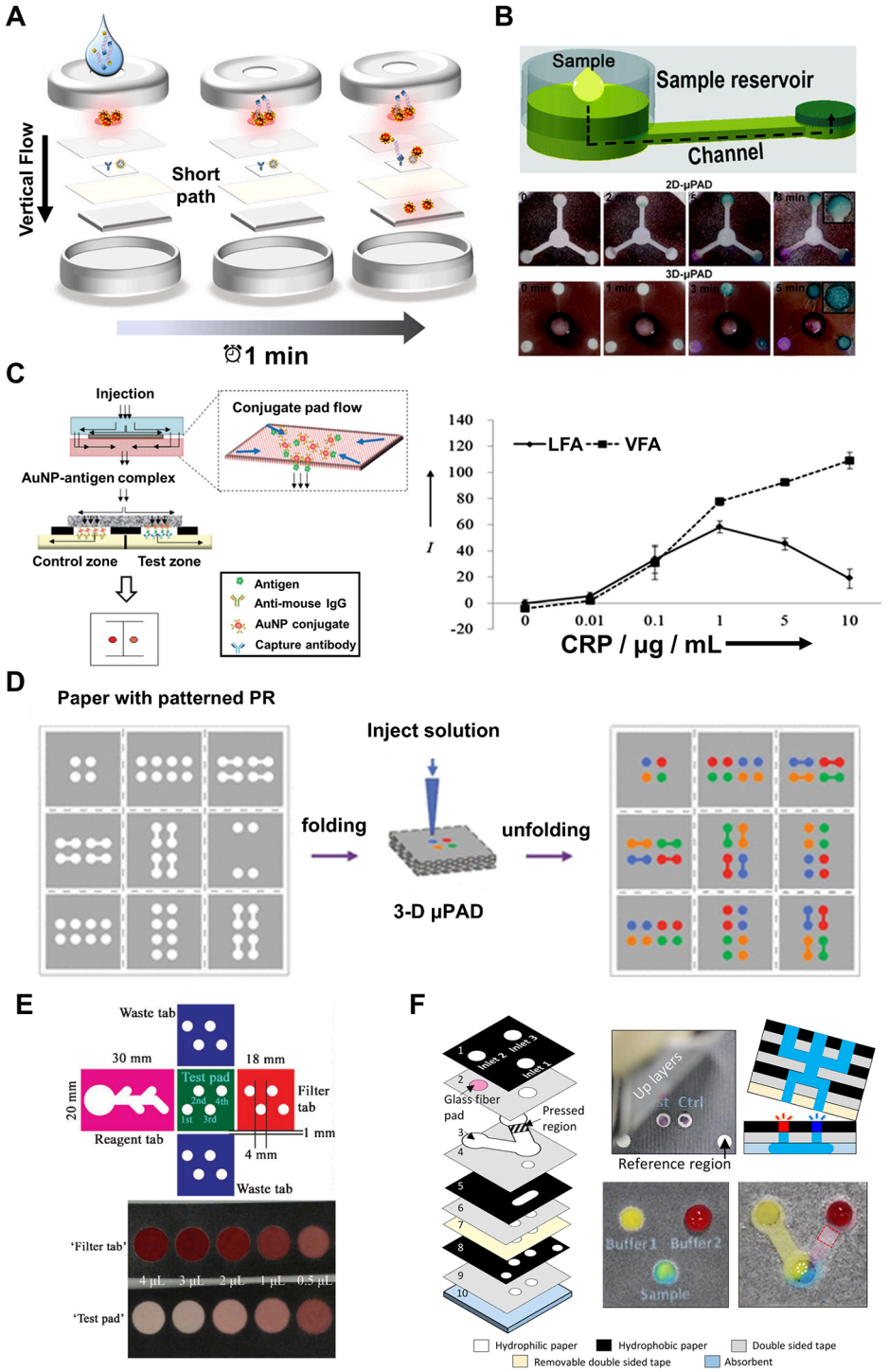

Figure 2. Comparison of lateral flow and vertical flow with illustrations of VF-μPADs in POCT. (A) Illustration of the shorter fluid path in VF-μPADs, enabling rapid fluid transfer through vertically stacked layers. This arrangement reduces assay time.[34] Reproduced with permission from ref (34). Available under a CC-BY license. Copyright 2021 MDPI. (B) Difference in color signal uniformity between LF-μPADs and VF-μPADs depending on flow direction.[37] Reproduced with permission from ref (37). Copyright 2019 American Chemical Society. (C) Effect of flow direction on assay performance. Schematic representation illustrating fluid division into two streams directed into the control and test zones, effectively mitigating the hook effect through vertical flow.[7] Reproduced with permission from ref (7). Copyright 2013 Royal Society of Chemistry. (D) Multiplexing in VF-μPADs achieved by folding and unfolding patterned paper with photoresist. This design allows simultaneous detection of multiple analytes within a compact device.[16] Reproduced with permission from ref (16). Copyright 2011 American Chemical Society. (E) Blood separation in VF-μPADs using a filtration layer. Reproduced with permission from ref (41). Copyright 2012 American Chemical Society. (F) Fluid control in VF-μPADs using multiple functional layers.[42] Reproduced with permission from ref (42). Copyright 2017 Elsevier B.V.

particular, the hook effect suppresses the true signal value, leading to lower-than-expected measurements that can result in both false negatives and inaccurate quantification at high analyte concentrations.[10] Multiplexing in LF-μPADs can lead to cross-reactivity between sequentially arranged test lines in a single fluid flow channel, making them prone to false positives

https://doi.org/10.1021/acssensors.5c00668
ACS Sens. 2025, 10, 3317−3339

and signal interference.[11,12,27−30] In LF-μPADs, incorporating additional analytes for multiplexed assays requires adding more test lines or spots, which in turn necessitates lengthening the device. This expansion leads to increased sample loss and dead volume, complicating both the maintenance of a compact design and the interpretation of results.[28] Furthermore, potential flow nonuniformity across different sections of an enlarged device can impact consistency, presenting challenges for achieving reliable diagnostics.[31]

LF-μPADs and VF-μPADs share fundamental structural components, including the sample pad, absorption pad, and NC membranes, which are crucial for fluidic management and reaction processes.[12,22,32,33] However, LF-μPADs primarily utilize horizontal flow paths with test and control lines for detection, whereas VF-μPADs operate along a vertical axis, using stacked layers or channels to guide fluid downward. This distinction enables VF-μPADs to support individual immunoreaction zones arrayed in parallel, in contrast to the line-based format in LFAs (Figure 1B), minimizing potential cross-talk. The vertical architecture of VF-μPADs addresses several limitations of LF-μPADs, offering advantages such as reduced assay durations,[34] enhanced multiplexing capabilities,[12,35] and minimized hook effect.[7,11,36] As illustrated in Figure 2A, the vertical flow configuration in VF-μPADs shortens the fluidic pathway compared to the lateral flow configuration, resulting in faster assay times, which makes them particularly advantageous for POCT.[34] Additionally, the ability to integrate multiple functional layers in VF-μPADs, such as separation, reagent storage, and detection, enhances their multiplexing potential and improves overall performance.[18,37,38]

VF-μPADs offer improved signal uniformity by ensuring consistent fluid distribution across detection zones, which enhances the reliability of the signal.[37,39] In LF-μPADs, the horizontal fluid flow causes the signals in the detection zone to shift toward the edges, often resulting in an uneven signal distribution across the detection zones.[37] Additionally, signal accumulation at the test line front can further distort signal intensity, affecting the accuracy and reproducibility of the assay, particularly in quantitative applications. Conversely, as the fluid moves directly downward through the layers, the vertical fluid flow in VF-μPADs eliminates signal nonuniformity issues, leading to a more uniform signal distribution in the detection zone. For instance, 3D geometries fabricated by 3D printing, which facilitate vertical fluid flow to the detection areas, can overcome the uneven colorimetric detection signals associated with horizontal fluid flows (Figure 2B).[37]

Additionally, the vertical flow configuration helps mitigate the hook effect, which arises when excessive antigen saturates the binding sites of capture/detection antibodies, preventing the formation of proper immunoassay complexes necessary for signal generation. Vertical flow addresses this issue by ensuring that the sample fluid is more evenly distributed across test spots within a short time frame, offsetting the imbalanced binding dynamics caused by excessive free antigen and ensuring accurate analyte detection even at high concentrations (Figure 2C).[7] VF-μPADs can be adapted for advanced assay operation by separating biomarker capture and detection antibody binding into distinct steps, offering a flexible approach to executing assays.[12,23,24] In this design, the antigen and detection antibody are delivered sequentially to the sensing membrane, which is pretreated with capture antibodies using separate top cases. This approach minimizes interference from excess antigens by isolating detection antibodies from antigen overload during the binding process. An alternative method for mitigating the hook effect combines multiplexed immunoreaction channels (e.g., spots with varying antibody concentrations and antigen/antibody mixtures) in VF-μPADs with advanced computational techniques (e.g., machine-learning-driven statistical feature selection). This system effectively identifies and excludes outlier data points caused by antigen saturation, thereby reducing false reporting and maintaining assay accuracy even at high antigen concentrations. Therefore, the vertical flow assay format enables greater flexibility in assay design, bypassing the hook effect and enabling accurate quantification across a wide range of analyte concentrations. These capabilities make VF-μPADs particularly advantageous for assays requiring high dynamic range sensitivity and reliable quantification.

Another notable advantage of VF-μPADs is their superior multiplexing capability.[11,12,39,40] The vertical flow enables the integration of multiple test regions within a compact device while avoiding the cross-reactivity typically observed in LF-μPADs.[35] Technologies such as hydrophobic wax printing and 3D printing, as shown in Figure 2D, allow the creation of compartments of test areas and prevent cross-contamination, thereby enabling the parallel analysis of multiple analytes.[12,16] This setup allows for the simultaneous detection of multiple analytes in a single test, making it ideal for complex diagnostics (Figure 2D).[16] While this multiplexing capability enables simultaneous detection of multiple analytes, it also presents challenges for signal interpretation. As the number of test spots increases, distinguishing individual signals by eye becomes more difficult. Therefore, VF-μPADs often require readers and image analysis software to capture and process results with sufficient accuracy and reproducibility. In contrast, LF-μPADs systems typically feature one or two test lines that are easily interpreted by the naked eye, making them more user-friendly and intuitive for rapid, qualitative assessments. This trade-off highlights the need for integrated digital tools in VF-μPAD platforms to fully leverage their multiplexing potential while maintaining usability.

VF-μPADs are also well-suited for handling complex samples, such as blood, as additional functional layers—such as filtration or flow control—can be incorporated to perform tasks like sample separation and impurity removal, as shown in Figure 2E.[41] This modularity is easily achieved by stacking or folding membranes, as depicted in Figure 2F, enabling sequential reagent delivery in multistep assays.[42]

Despite these advantages, VF-μPADs also present some challenges. Their fabrication requires precise alignment and contact between layers to ensure consistent fluid flow and accurate sample transfer and prevent potential reagent or sample leakage.[12] Misalignments can lead to uneven flow and compromise performance. Additionally, the intricate fabrication process of VF-μPADs requires precise deposition of multiple test spots within a single membrane. This often involves multiple dispensing nozzles and stringent quality control measures, which further increase production costs compared to LF-μPADs.[43,44] However, with the integration of diverse paper materials alongside scalable fabrication pipelines similar to those used for LF-μPADs, VF-μPADs can be reliably scaled up with consistent accuracy in a commercial setting. Ease of operation/usability is also a concern, as VF-μPADs may require more operational steps compared to LF-μPADs, depending on the platform and application.[39,42] Some VF-μPADs are designed such that the sensing region is always

https://doi.org/10.1021/acssensors.5c00668
ACS Sens. 2025, 10, 3317−3339

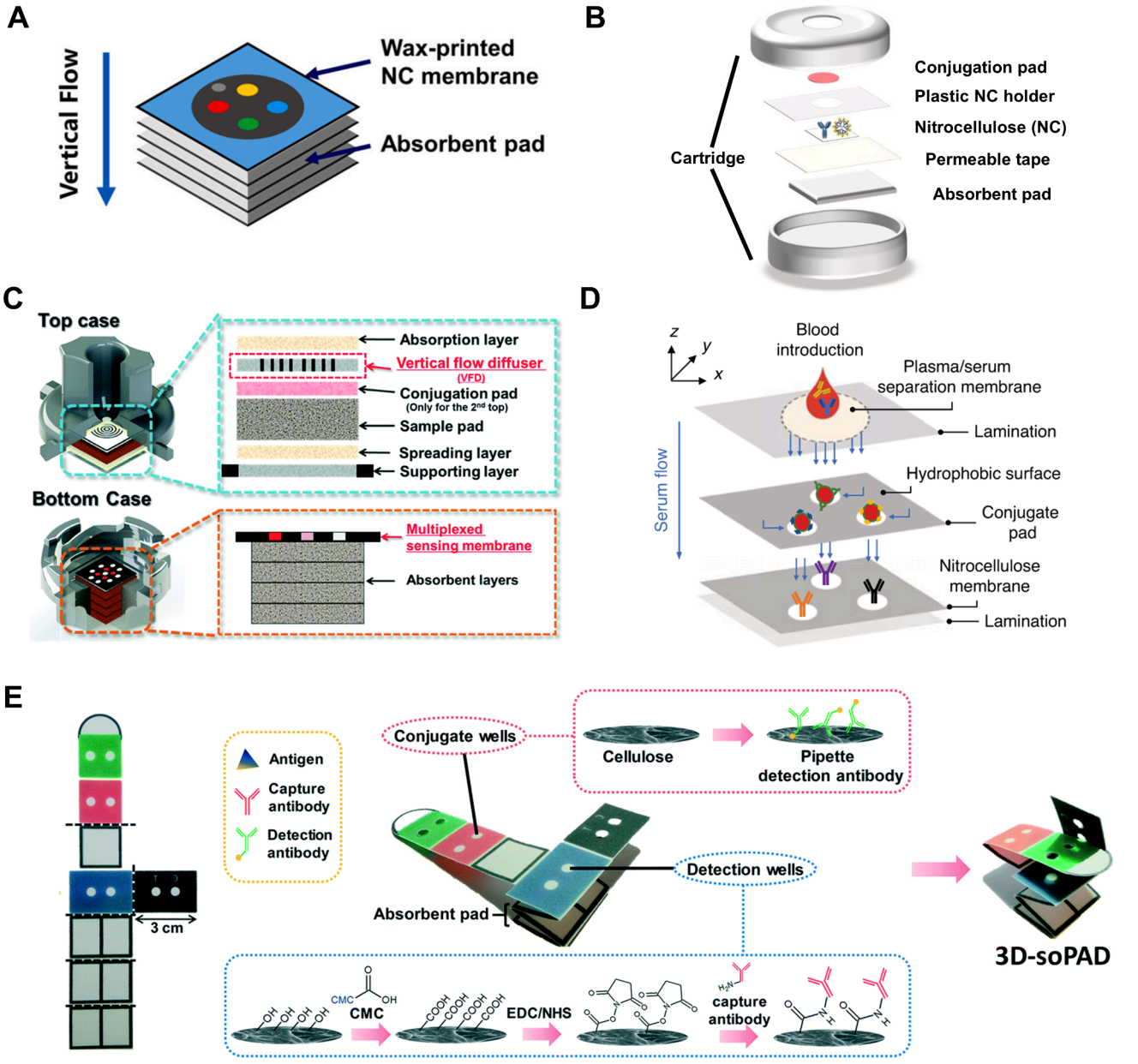

Figure 3. Structural components and configurations of VF-μPADs for enhanced diagnostic performance in POC applications. (A) Basic structure of a VF-μPAD consisting of multiple wax-printed layers, including a NC membrane for detection and an absorbent pad.[14] Reproduced with permission from ref (14). Copyright 2023 Elsevier B.V. (B) Schematic showing the inclusion of a conjugation pad in VF-μPADs. Cross-sectional illustration of the conjugation pad with in the layered structure.[34] Reproduced with permission from ref (34). Available under a CC-BY license. Copyright 2021 MDPI. (C) Integration of a vertical flow diffusers (VFDs) to ensure uniform fluid distribution across the sensing membrane (Left). Schematic of a VF-μPAD with VFD included, illustrating how fluid flow is directed evenly (Right).[12] Reproduced with permission from ref (12). Copyright 2019 Royal Society of Chemistry. (D) Use of a separation membrane for sample filtration in complex biological samples. The separation membrane, placed above the conjugation pad, filters out larger debris, such as cells and proteins, before they reach the sensing layers.[47] Reproduced with permission from ref. (47). Available under a CC-BY license. Copyright 2023 Springer Nature. (E) Single-membrane VF-μPAD design for simplified fabrication. A single cellulose membrane functions as both the conjugation pad and sensing membrane, reducing the need for complex layer alignment.[48] Reproduced with permission from ref (48). Copyright 2019 Royal Society of Chemistry.

exposed,[14] allowing real-time visualization of signals, while others remain closed during the assay operation,[20,22,24] with the reaction region only revealed at the end. Exposed sensing configurations enable continuous signal monitoring and are particularly advantageous when kinetic information is required. However, since the sensing membrane is placed at the top layer, these devices often cannot accommodate intermediate functional layers such as conjugation or filtration pads. As a result, sample pretreatment or premixing with detection reagents is typically necessary.[14] Conversely, closed configurations place the sensing membrane within internal layers, which prevents real-time monitoring but allows greater integration of functional layers. These designs enable direct sample loading without pretreatment, improving usability and minimizing user error, especially in point of care (POC) settings.[21] Therefore, VFAs may be limited to end-point assays rather than enabling continuous monitoring. However, since most POC tests require end-point measurements and rapid

https://doi.org/10.1021/acssensors.5c00668
ACS Sens. 2025, 10, 3317−3339

results, the faster sample-to-result time for the VF-μPADs compared to that for the LF-μPADs provides a significant advantage.

DESIGN AND FABRICATION OF VF-μPADs

Fabrication of VF-μPADs. *Structural Components.* VF-μPADs consist of multiple layers of porous substrates, each carefully engineered to perform a specific function within the assay operation (Figure 3). By controlling the fluid flow, these structural components ensure repeatable and accurate detection of target analytes, while maintaining a compact, user-friendly format ideal for POC applications.[35,45] The main structural components include the sample layer, conjugation pad, sensing membrane, and absorbent pad. Additionally, functional layers such as flow diffusers and separation membranes enhance performance by improving fluid control and sample processing.

A critical component of VF-μPADs is the sensing membrane, typically made of NC or other high protein-binding materials. These membranes are well-suited for immobilizing antibodies or other capture agents, enabling efficient binding of target analytes. To facilitate multiplexed reactions, planar membranes are often patterned using techniques such as wax printing or 3D printing to create parallel test zones.[12] These test zones minimize variability by incorporating multiple technical replicates and enhance diagnostic sensitivity by enabling the detection of multiple disease-associated analytes.[46]

Beneath the sensing membrane, VF-μPADs contain multiple absorbent pads that act as a sink for excess fluid, ensuring continuous fluid flow throughout the assay and preventing backflow toward the sensing membrane (Figure 3A).[14] These absorbent pads are critical for driving fluid flow because they create the necessary capillary action (e.g., wicking) to pull the fluid down from the sensing membrane. The sensing membrane remains exposed for easy imaging after assay completion by positioning the absorbent pads underneath.

To visualize the reaction process during assay incubation, prelabeled detector molecules are evenly distributed across the sensing membrane to bind the target analyte. To reduce liquid handling steps, VF-μPADs incorporate a dried conjugation pad preloaded with stabilized detection molecules within a porous substrate, positioned above the sensing membrane (Figure 3B).[34] Upon contact with the sample or buffer, the conjugation pad releases these molecules, facilitating automated reagent delivery. However, larger sensing membranes may encounter challenges related to fluid flow uniformity, potentially leading to inconsistent sensor performance.[12]

To address fluid flow uniformity issues, vertical flow diffusers (VFDs) can be integrated to distribute fluids evenly across the sensing membrane, ensuring consistent signal intensity across the entire sensing area (Figure 3C).[12] These diffusers are fabricated by patterning concentric hydrophobic rings that guide the fluid horizontally before directing it vertically. Essentially, this design transforms the spherical fluid front into a planar plug flow, thereby enabling a uniform flow rate across the sensing membrane. Without this diffuser, the assay reagents would instead congregate in the center, leading to the inactivation of peripheral test zones and a decrease in signal consistency. By integrating VFDs, the variation in flow intensity is minimized, reducing inconsistencies between the center and edges of the membrane. This leads to a more homogeneous reaction environment, improving the coefficient of variation (CV) of signal intensities and enhancing overall assay accuracy.[12]

When working with complex biological samples, such as whole blood or saliva, additional challenges emerge owing to the presence of cellular debris, red blood cells, and proteins that can interfere with assays. These components can lead to signal variability, reduced sensitivity, and membrane obstruction, impeding fluid flow. To address these issues, some research groups have developed methods to integrate separation membranes directly into the VF-μPAD design. For instance, Boumar et al.[47] incorporated a separation membrane above the conjugation pad (Figure 3D), which functions as a filter to remove larger biological debris, such as cells and proteins, from the sample before it reaches the downstream layers. The strategic placement of this separation membrane significantly improves signal uniformity and enhances assay sensitivity by minimizing interference from extraneous components in the sample. These membranes enable VF-μPADs to handle more complex specimens directly, eliminating the need for extensive preprocessing and streamlining the diagnostic process. The ability to use unprocessed samples, such as whole blood or saliva, enhances the practicality of VF-μPADs in POC settings, offering faster and more reliable diagnostics in resource-limited environments.

Cartridge or housing plays a crucial role in VF-μPADs by providing structural support to the layered components and protecting the sensor from environmental contamination or mechanical damage during handling. Many VF-μPAD designs incorporate cartridges to ensure precise alignment of the functional layers with predefined sample loading ports, improving flow uniformity.[12,34] Advanced cartridges may include microchannels or passive valves to control fluid distribution, further enhancing reproducibility and minimizing user error. In addition, the housing design directly affects the sensing performance. For instance, optimizing the compressibility of stacked membranes improves the signal uniformity by ensuring better contact between the layers for consistent fluid flow.[22] However, excessive compression can obstruct fluid movement by damaging the original porous structure of the membrane layers, highlighting the need for precise engineering to achieve an optimal balance. In research settings, housings are often fabricated using 3D printing for rapid prototyping, whereas large-scale production may rely on injection molding to balance efficiency and cost.

While incorporating multiple functional membranes in VF-μPADs can enhance performance by optimizing each layer for specific tasks—such as conjugation, sensing, or filtration—this approach can also complicate the fabrication process. The need to precisely align and stack membranes adds complexity to assembly, making the process labor-intensive and more challenging to scale. Consequently, simpler designs that rely on a single membrane to perform multiple functions within a device have emerged. In these simpler VF-μPAD designs, a single membrane can function as the conjugation pad, sensing membrane, and absorbent layer simultaneously. This is often the case in folding-based VF-μPADs, where the membrane is folded or patterned to create the necessary vertical flow channels for fluid transport. These designs reduce the fabrication complexity while maintaining the advantages of vertical flow using a single membrane—typically a versatile material such as cellulose. The flexibility of cellulose allows it to serve as a fluid transport channel while providing sufficient surface area for biomolecule immobilization and absorption of

https://doi.org/10.1021/acssensors.5c00668
ACS Sens. 2025, 10, 3317−3339

Table 1. Common Materials Used in VF-μPADs

Material	Properties	Common Uses in VF-μPADs	Advantages	Disadvantages	Ref.
Cellulose	Porous, hydrophilic, flexible, affordable	Sensing membrane, separation, absorbent pad	Excellent capillary action, versatility, durability, low cost	Less effective for protein binding compared to NC	58−63
Nitrocellulose (NC)	High protein-binding capacity, uniform pore structure	Sensing membranes	Superior sensitivity and specificity, consistent fluid flow	Expensive, less flexible, not suitable for complex folding structures	14, 21, 23, 64−66
Glass Fiber	High porosity, smooth capillary flow	Conjugation pad	Even release of detection molecules, prevents blockages, supports smooth fluid movement	Generally, more expensive than cellulose	34, 40, 66−69
Cotton Fiber	Excellent fluid retention, strong absorbency	Absorbent pad	Rapid and high-volume absorption, maintains dry sensing area	Bulkier compared to other absorbent materials	12, 70−72
Polysulfone	Asymmetric pore size, selective permeability	Separation membranes for plasma separation	Efficient filtration of red blood cells and unwanted components, high selectivity	More expensive, may require specialized fabrication techniques	18, 56, 57

excess fluids. Such designs are particularly appealing for low-cost diagnostics, for which simplicity, affordability, and ease of manufacturing are critical (Figure 3E).[48]

Scalability remains a critical challenge for the widespread adoption of VF-μPADs. Addressing this issue requires optimizing the fabrication techniques to ensure that large-scale production does not compromise device performance and reliability. Future developments will focus on creating mass-production methods, integrating automated manufacturing processes, and utilizing cost-effective and sustainable materials similar to those used in the large-scale production of LFA tests. By utilizing automated droplet dispensers and advanced reagent coating techniques, VF-μPADs can be enhanced to support greater multiplexing. This enables the measurement of additional biomarkers, such as an individual's entire immune repertoire, in a single test. Once VF-μPADs can be produced efficiently and economically in large quantities, their applications can be extended to both in vitro diagnostics and environmental monitoring.

Material Selection. Material selection is crucial in the construction of VF-μPADs, as it directly impacts the device's fluid management, interaction with biological samples, and overall diagnostic accuracy. Paper is widely used as a substrate for these devices owing to its porous nature, hydrophilic properties, and low cost.[35,49] The specific characteristics of the paper, such as its thickness, fiber density, and pore size, are carefully chosen to optimize the performance of the device. These factors significantly affect fluid transport, sample-reagent interactions, and signal generation within VF-μPADs.

Cellulose is one of the most commonly used materials in VF-μPADs. Its widespread use can be attributed to its excellent material properties, affordability, and versatility, making it ideal for various functions, including sensing membranes, separation, and absorbent pads.[5] Cellulose-based materials, such as filter paper and chromatography paper, are often preferred for their capillary action, which enables fluid flow without the need for external pumps.[5] Additionally, cellulose is more flexible and durable than other materials, such as NC, making it easier to incorporate into designs that require folding or origami structures.[34] However, while cellulose can serve multiple functions, it may not always deliver the same optimized performance as materials specifically designed for certain tasks. For instance, although cellulose can be used in sensing applications, it is less effective than NC at binding proteins.[50] Additionally, while cellulose has strong absorbent capabilities, it may not offer tailored fluid management properties of cotton fibers.

In contrast, NC is commonly chosen for sensing membranes because of its exceptional ability to bind proteins and immobilize antibodies or other bioreceptors.[51] Its high protein-binding capacity makes it the material of choice in applications where sensitivity and specificity are critical.[50] Uniform pore structure of NC ensures consistent fluid flow across the membrane, enhancing the interaction between the sample and bioreceptors, which leads to more accurate detection. Although NC offers superior performance in capturing target analytes, it is generally more expensive and less flexible than cellulose, making it less suitable for low-cost devices or complex folding structures.[41]

The conjugation pad plays a crucial role in storing and releasing prelabeled detection molecules, such as nanoparticles or fluorescent markers.[52−54] Glass fiber and Cytiva CF7 are the preferred materials for conjugation pads because of the high porosity, which allows them to store detection reagents and release them evenly as the sample flows through the device. This uniform release is vital for ensuring a consistent reaction between the sample and detection molecules, directly affecting the reliability and reproducibility of the assay.

The absorbent pad is another critical component responsible for managing excess fluid in the system and ensuring that the assay progresses smoothly without overflow or backflow, which could lead to false positives.[53−55] Materials like cotton fiber, commonly used in Whatman grade 707 or Ahlstrom grade 222, are highly effective for this purpose. The excellent fluid retention properties of the cotton fibers ensure that excess fluid is quickly absorbed, keeping the sensing area dry and free from interference. In addition, cellulose-based absorbent pads can be used to draw fluid consistently through the device at high wicking rates, maintain capillary action, and ensure proper assay function. Both cotton fibers and cellulose offer strong fluid management capabilities, with cotton often being preferred for rapid and high-volume absorption.

In more complex devices, additional functional layers are incorporated to handle specialized tasks, such as blood filtration.[18,56,57] Polysulfone membranes are commonly used in these cases, particularly for plasma separation, because of their asymmetric pore size structure, which efficiently filters out red blood cells and other unwanted components, allowing only plasma to pass through the detection zone with reduced clogging.[18,56] Filtration can be important in blood diagnostics to ensure that the sample is free of interference before analysis.

In summary, the selection of materials in VF-μPADs is crucial for optimizing fluid management, enhancing interaction with biological samples, and ensuring accurate diagnostic results. Cellulose is favored because of its versatility and cost-

https://doi.org/10.1021/acssensors.5c00668
ACS Sens. 2025, 10, 3317−3339

effectiveness, which make it suitable for multiple functions within devices. NC offers superior protein-binding capabilities and enhances assay sensitivity and specificity, but at a higher cost and reduced flexibility. Glass fiber is a good choice for the conjugation pad, providing a uniform release of detection molecules and supporting consistent fluid flow, whereas cotton fiber excels in managing excess fluid owing to its high absorbency. Polysulfone membranes are preferred for specialized applications such as blood plasma separation because of their selective permeability and efficient filtration properties.

The choice of the material is further influenced by the device fabrication method, which is discussed in detail in the following section. The stacking of different paper layers benefits from the cumulative advantages of the different paper layers to configure an assembly that integrates the individual functions, optimize performance. By contrast, folding- or origami-based designs rely on the multifunctionality of cellulose, allowing for simpler and more compact device architectures. This strategic material selection ensures that VF-μPADs can perform complex biochemical assays reliably while maintaining user-friendly and cost-effective designs. Table 1 summarizes the common materials used in VF-μPADs, outlining their properties, advantages, and disadvantages, thereby emphasizing the role of each material in supporting specific device functionalities.[12,14,18,21,23,34,40,56−72]

Fabrication of VF-μPADs. There are three major methods described for fabricating VF-μPADs: folding/origami,[16,17,19,41,59,60,62,67−69,73−78] stacking,[12,14,21,23,40,47,57,64,65,71,72,79] and 3D printing.[15,18,37,38,80] Each of these fabrication methods offers the flexibility to use various porous membrane materials, depending on the specific design and functional requirements of the device. The choice of the fabrication method can profoundly influence not only the materials selected but also the overall performance, complexity, and scalability of the device. For example, stacking methods allow the incorporation of specialized membranes, each optimized for distinct functions. In contrast, folding/origami approaches, which are typically limited to a single multifunctional membrane, offer the benefits of simplified fabrication and reduced assembly time. Meanwhile, 3D printing enables precise material integration but introduces challenges related to fabrication complexity.

The following sections explore the principles, advantages, and limitations of each fabrication method, beginning with the stacking method, followed by folding and origami, and finally, 3D printing.

VF-μPAD Fabrication by Folding. The folding/origami method is one of the simplest and most widely used fabrication techniques for VF-μPADs.[16,17,41,67,81,82] This method typically involves the use of a single type of membrane, onto which hydrophobic patterns are created using techniques such as wax printing or laser patterning. The membrane is then folded into a three-dimensional structure to form the functional layers of the device. Due to the use of a single membrane, cellulose membranes are most commonly employed because of their versatility and ability to perform multiple functions, such as fluid transport, sensing, and absorption. This makes the folding/origami method suitable for a wide range of diagnostic applications, including the detection of antibodies,[19,41,73] proteins,[16,62,78] nucleic acids,[17,77,83] bacteria, and viruses.[67−70,75] The flexibility of cellulose makes it an ideal choice for general-purpose diagnostics in various fields.

The primary advantages of the folding/origami method are simplicity and ease of fabrication. The process requires fewer materials and less precision than more complex methods such as stacking, making it an attractive option for low-cost, scalable production. Additionally, the folding method is cost-effective, allowing for the rapid and inexpensive production of VF-μPADs, which is particularly beneficial in POC settings and resource-limited environments.

However, the reliance on a single membrane introduces limitations. Because the folding/origami method does not easily accommodate the use of membranes optimized for specific functions (e.g., antibody immobilization or filtration), its performance may be lower than that of methods that allow the use of specialized membranes such as NC or polysulfone. Although cellulose is flexible and multifunctional, it may not offer the same level of sensitivity or separation efficiency as specialized materials.

To address these limitations, some adaptations of the folding/origami method involve the integration of additional functional membranes. For example, glass fiber membranes, which have low protein-binding affinity, can be attached to the cellulose membrane by wax printing to enable purified DNA extraction after cell lysis.[68] In this variation, the folded structure can include different sections dedicated to separation, flow control, and detection, allowing the device to handle more complex samples while maintaining the simplicity and low cost of the folding method.[83]

VF-μPAD Fabrication by Stacking. The stacking method is also a widely used fabrication approach for VF-μPADs, where multiple layers of membranes, each with a distinct function, are stacked on top of each other to form the device.[21] VF-μPADs fabricated using the stacking method are typically constructed by connecting patterned individual layers—created through techniques such as wax printing—using adhesive tape or by compressing the layers into a cassette or case to form a cohesive structure.[6,12,14,21,23,57,71] This method allows for the integration of various functional layers, such as the sensing membrane, conjugation pad, filtration membrane, flow control layer, and absorbent pad, all of which are crucial for ensuring optimal performance in VF-μPADs. In many cases, adhesive materials such as double-sided foam tapes are used to maintain alignment of the layers and prevent fluid leakage. For instance, food-grade polyethylene foam tapes have been employed to secure the outer layers of the device, functioning simultaneously as structural support and as a gasket to avoid reagent bypass. However, the use of adhesive tape is not mandatory. In some designs, wax printing or screen-printed hydrophobic adhesives can provide sufficient bonding between layers without additional materials. The choice of adhesive depends on the membrane properties and assay requirements; nonetheless, biocompatible materials are preferred when tapes are used in proximity to the sensing region.

A key advantage of the stacking method is its ability to use different types of membranes optimized for each function. For example, NC membranes are commonly used as sensing layers because of their high protein-binding capacity, whereas cellulose membranes offer durability, high chemical resistance, and excellent liquid-handling capabilities.[12,14,66] Additionally, glass fiber membranes are used as conjugation pads to store and release detection reagents,[34,40] whereas cotton fiber or cellulose pads are used for absorption.[12,70] This flexibility allows for the creation of high-performance μPADs that are specifically tailored for various diagnostic applications.

https://doi.org/10.1021/acssensors.5c00668
ACS Sens. 2025, 10, 3317−3339

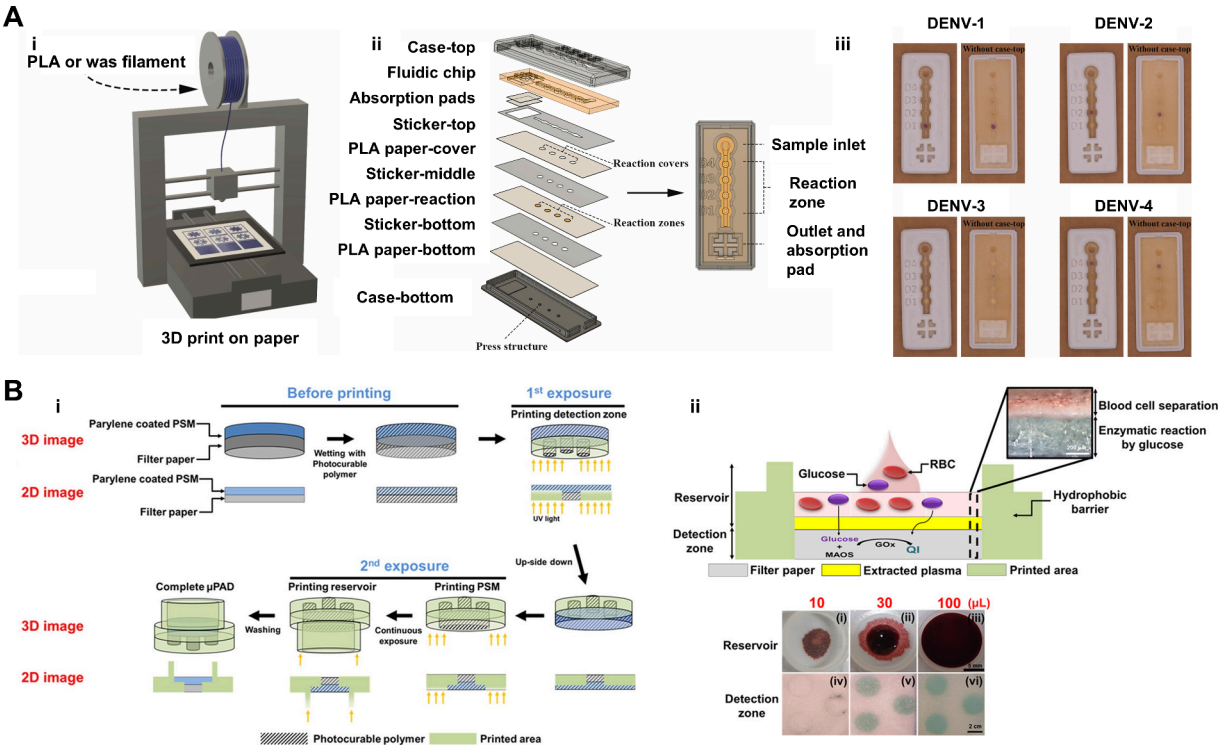

Figure 4. 3D Printing techniques in the fabrication of VF-μPADs for POCT. (A) FDM approach for VF-μPAD fabrication using PLA and wax filaments: (i) Illustration of an FDM 3D printer depositing PLA and wax filaments onto Whatman chromatography paper to create hydrophobic barriers; (ii) view of the VF-μPAD layers produced by FDM, including the sample inlet, reaction zones, and absorbent pad; and (iii) VF-μPADs for dengue virus serotype detection using cell-free reactions.[80] Reproduced with permission from ref (80). Copyright 2021 Elsevier B.V. (B) DLP 3D printing approach for VF-μPAD fabrication with integrated plasma separation functionality: (i) Schematic of DLP printing setup showing the integration of a parylene C-coated PSM within a photocurable polymer matrix and (ii) illustration of the wetting of the plasma separation membrane (PSM) and the corresponding color generation in the detection zone using 10, 30, and 100 μL of whole blood containing 5 mM glucose.[18] Reproduced with permission from ref (18). Copyright 2019, American Chemical Society.

The stacking method also facilitates the addition of specialized functional layers, such as filtration and flow control membranes.[57] These layers enable the handling of complex samples and the performance of sophisticated assays requiring sample preprocessing, such as filtration or flow regulation, thus enabling VF-μPADs to detect a wide range of analytes, including proteins, nucleic acids, bacteria, antibodies, and ions, from various body fluids.

However, stacking poses several challenges. These layers are often connected or aligned using adhesive tape or external holders, which complicates the fabrication process. This can introduce issues such as inconsistent layer alignment or interference with the fluid flow owing to uneven adhesion or tape residue. Proper alignment and contact between the layers are crucial for the device to function correctly. Misalignment or weak contacting can result in uneven fluid flow or incomplete sample transfer, compromising assay accuracy. Ensuring strong adhesion and consistent membrane contact after assembly is essential for maintaining the uniform flow required for reliable multiplexed diagnostics. In most reported VF-μPADs, layer alignment is performed manually during prototyping, often with the help of alignment pins or visual guides. While this is feasible for laboratory-scale fabrication, it introduces variability and is not ideal for mass production. To enable scalable manufacturing, semiautomated or roll-to-roll alignment systems, similar to those used in LFA production lines, may be adopted to ensure consistent and reproducible assembly of multilayer devices.

Despite the flexibility and performance benefits of this stacking method, its complexity introduces challenges for high-throughput production. The precision required for membrane placement and the reliability of connections between the layers require careful attention during fabrication. Although this method allows the creation of highly sensitive and customizable devices, the increased labor and manufacturing costs must be carefully balanced against its advantages. In high-throughput settings, these complexities may increase costs; however, advancements in machine-based and automated robotic assembly techniques may enable the efficient scaling of stacking methods. Conversely, on smaller scales, inaccuracies may result from reliance on manual control, underscoring the need for precise methodologies to ensure reproducibility and internal controls for low-volume production.

VF-μPAD Fabrication using a 3D Printing Method. Recent advances in 3D printing have enabled the fabrication of VF-μPADs with enhanced precision and functionality. Two distinct approaches—fused deposition modeling (FDM) with polylactic acid (PLA) filaments[80] and wax/resin-based digital light processing (DLP)[15,18,37,38,84]—have been utilized to create intricate layered devices for POC diagnostics. These techniques allow the integration of hydrophilic channels, hydrophobic barriers, and functional layers, thereby facilitating precise control of fluid dynamics in complex diagnostic assays. Because of these features, 3D printing enables the efficient fabrication of integrated monolithic devices, streamlining the production process for advanced diagnostic applications.

https://doi.org/10.1021/acssensors.5c00668
ACS Sens. 2025, 10, 3317−3339

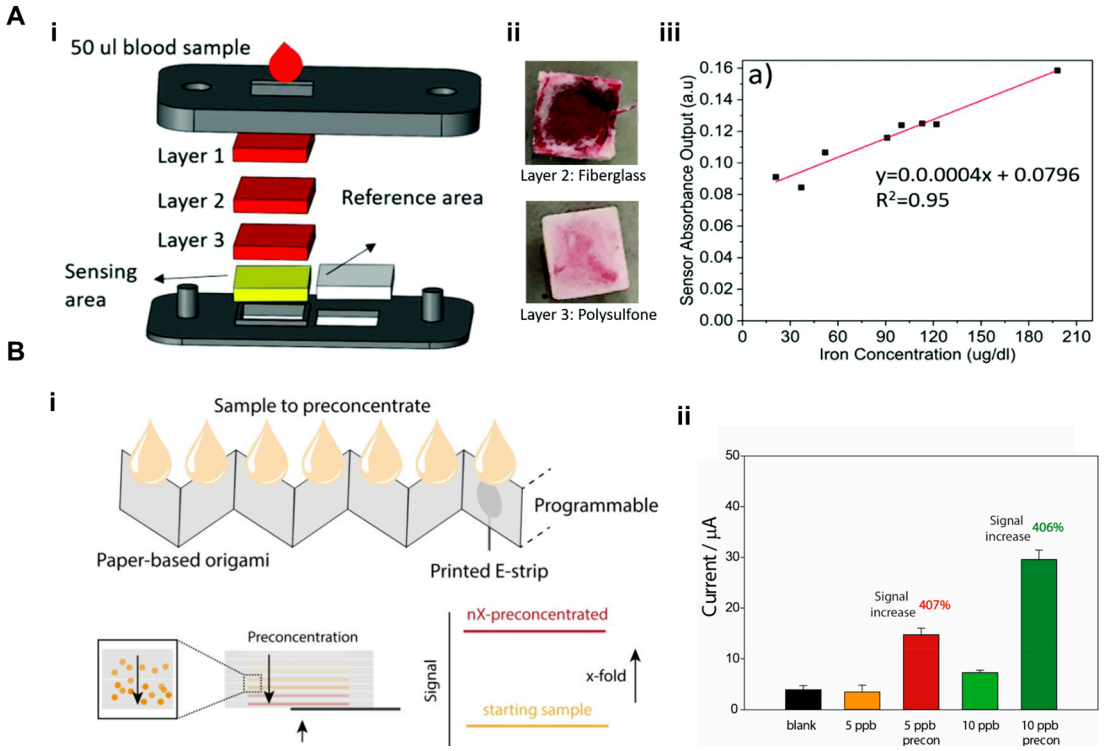

Figure 5. Applications of VF-μPADs for noninfectious diseases. (A) VF-μPADs for POC measurement of iron from whole blood: (i) Sensor strip consists of four sandwiched membranes and hosts 50 μL of whole blood sample; (ii) GF membrane which acts as a primary filtration layer (top) while asymmetric polysulfone membrane which acts as a secondary filtration layer (bottom); and (iii) calibration curve for blood ion detection exhibited a slope of 0.0004 with a coefficient of determination (R^2) of 0.95.[56] Reproduced with permission from ref (56). Copyright 2021 Royal Society of Chemistry. (B) VF-μPADs fabricated by origami method for programmable multifold analyte preconcentration: (i) Schematic representation and assembly of the 3D paper-based origami device for programmable analyte preconcentration and (ii) histograms showing a 407% and 406% signal increase for 5 and 10 ppb glucose, respectively, after preconcentration.[90] Reproduced with permission from ref (90). Copyright 2024 American Chemical Society.

The first method, introduced by Suvanasuthi et al.,[80] employs an FDM 3D printer to deposit PLA and wax filaments onto Whatman chromatography paper (CHR), forming hydrophobic barriers that regulate the fluid flow within the device (Figure 4Ai and 4Aii). Custom patterns are printed directly onto a paper substrate and heated to embed hydrophobic barriers into the fibers, tailoring the device for specific diagnostic applications. The printed device was used to detect dengue virus serotypes via cell-free reactions (Figure 4Aiii). This approach offers flexibility, enabling rapid prototyping of multiplexed diagnostic zones, making it particularly suitable for low-cost, scalable POCT in resource-limited settings. However, challenges such as the lower resolution of printed barriers and batch-to-batch variability may affect the precision and reproducibility of fluid flow control, particularly when dealing with biological samples.

In a more integrated approach, Park et al.[18] demonstrated the fabrication of a VF-μPAD using DLP 3D printing, incorporating a PSM directly into the device structure (Figure 4Bi). In this method, a polysulfone membrane coated with parylene C was used to separate plasma from whole blood. The PSM was embedded within a photocurable polymer matrix during printing, resulting in a monolithic structure with integrated filtration and detection layers. This approach eliminates the need for additional bonding or stacking steps to ensure precise alignment of all functional components. The device was used to detect glucose in whole blood, with the PSM efficiently filtering out red blood cells and enabling reliable colorimetric detection (Figure 4Bii). DLP printing offers notable advantages, particularly its ability to integrate multiple functional layers into a single, cohesive device without requiring additional assembly. However, this method necessitates specialized equipment and materials, such as DLP printers and photocurable polymers, which can increase both production complexity and cost.[84] Furthermore, the use of a parylene C coating to protect the PSM from curing introduces an additional step in the fabrication process.[18]

Overall, these 3D printing techniques represent substantial advancements in the fabrication of VF-μPADs. The FDM method, which emphasize rapid prototyping and cost efficiency, is particularly suitable for resource-limited settings where affordable and quick diagnostics are critical. By contrast, the DLP technique provides higher precision and integrated functionality, making it more appropriate for applications requiring complex sample processing, such as plasma separation. Both approaches highlight the potential of 3D printing to produce customizable, multifunctional VF-μPADs capable of addressing the growing demand for POC diagnostics.

APPLICATION OF VF-μPADs

In Vitro Diagnostics. The versatile structural features and advantages of VF-μPADs enable their application in a wide range of in vitro diagnostics.[24,85−100] For instance, they facilitate the detection of antigens,[74,13,23,24,48] and nucleic acids[63,85,89] for infectious disease diagnosis, as well as small

https://doi.org/10.1021/acssensors.5c00668
ACS Sens. 2025, 10, 3317−3339

molecules such as glucose, ammonia, iron, and protein biomarkers for noninfectious disease diagnosis.[20,56,86−88,90]

Small Molecule Detection. VF-μPADs are well-suited for small molecule detection in POCT due to their ability to handle complex samples and enable multiplexed detection of several biomarker panels directly from biological fluids such as blood[56] and sweat,[90] without requiring extensive pretreatment.

For example, Serhan et al.[56] developed a VF-μPAD for the rapid and cost-effective quantification of total iron in whole blood (Figure 5A). This device incorporates a layered membrane design, including GF as the primary filtration layer and asymmetric polysulfone as the secondary filtration layer, which effectively separates the plasma from the cellular components (Figure 5Ai and 5Aii). This separation enables a direct colorimetric reaction between transferrin-bound iron and ferene, producing a measurable color change that can be captured and analyzed using a smartphone application. The system achieves a detection time of 5 min with a sensor cost of less than 10 cents per test. Although the smartphone-based calibration curve showed a slope of 0.0004 AU μg^{-1} dL^{-1} with an R^2 value of 0.95, which indicates a moderate correlation, the original study acknowledged that samples were artificially diluted and recommended future validation using clinically relevant samples (Figure 5Aiii). Thus, while this device demonstrates the potential of VF-μPADs for point-of-care iron screening, further development is needed to ensure clinical reliability. Nevertheless, its portability and low sample volume requirement (50 μL from a finger-prick) make it particularly well-suited for resource-limited settings, addressing the global need for accessible and effective iron deficiency diagnostics. This study highlights the potential of VF-μPADs in advancing POCT for noninfectious disease management.

To further enhance analytical performance, VF-μPADs can improve sensitivity by preconcentrating samples or employing electrochemical detection methods. In particular, biological samples like sweat contain biomarkers at significantly lower concentrations compared to blood, necessitating heightened detection sensitivity.[90] For instance, Kalligosfyri et al.[90] developed a VF-μPAD with electrodes that leverage a vertical flow mechanism to preconcentrate analytes, such as glucose, directly onto the bottom sensing layer (Figure 5Bi). The preconcentrated glucose was then electrochemically detected using integrated screen-printed electrodes on the bottom layer. The device utilized chronoamperometric detection, where glucose oxidase catalyzed the oxidation of glucose, producing H_2O_2, which was subsequently electrocatalytically reduced by Prussian blue on the electrode surface to generate a measurable current. This preconcentration significantly enhanced the sensitivity of the detection process, allowing glucose detection in sweat samples at concentrations as low as 0.1 mM, with up to a 300% increase in signal response (Figure 5Bii).

Protein Biomarkers for Noninfectious Diseases. Protein biomarkers play a crucial role in the diagnosis and management of noninfectious diseases and serve as indicators of physiological and pathological processes within the body. For example, C-reactive protein (CRP) is a versatile biomarker that can be used to assess systemic inflammation at high concentrations and to evaluate cardiovascular disease (CVD) risk at low concentrations, similar to high-sensitivity CRP (hsCRP). Cardiac-specific proteins such as troponins, creatine kinase-MB (CK-MB), myoglobin, and heart-type fatty acid-binding protein (FABP) are widely used to diagnose and monitor cardiovascular conditions. These biomarkers provide valuable insights into disease progression, treatment efficacy, and overall health. The ability of VF-μPADs to integrate multiplexed detection and rapid analysis positions them as an effective platform for measuring these biomarkers in POC settings. By offering fast, accurate, and cost-effective testing, VF-μPADs have the potential to revolutionize diagnostics for noninfectious diseases, particularly in resource-limited settings.

Goncharov et al.[21] developed a POC diagnostic platform that integrates a paper-based fluorescence vertical flow assay (fxVFA) with deep learning algorithms. This system enables the simultaneous quantification of three cardiac biomarkers—myoglobin, CK-MB, and FABP—using a low-cost mobile reader. The fxVFA requires only 50 μL of serum and delivers results in less than 15 min. The incorporation of neural network-based inference enhances the accuracy of biomarker concentration quantification, achieving limits of detection below 0.52 ng/mL for all three biomarkers with minimal cross-reactivity. Blind testing with 46 individually activated cartridges demonstrated a high correlation with ground truth concentrations, exhibiting linearity greater than 0.9 and a CV below 15%. The competitive performance of this platform, combined with its inexpensive paper-based design and hand-held footprint, is promising for expanding the access to diagnostics in resource-limited settings.

To address the challenges to POC diagnostics posed by low-abundance blood biomarkers like cardiac troponin I (cTnI), the adoption of VF-μPADs has driven significant advancements in high-sensitivity assays. cTnI is a critical biomarker for assessing myocardial injury, necessitating detection capabilities at the pg/mL level for accurate identification of individuals with cardiac disease. To achieve the required sensitivity for high-sensitivity cTnI detection, emerging VF-μPADs leverage signal amplification strategies (e.g., colorimetric nanoparticle amplification) or advanced sensing modalities (e.g., chemiluminescence).

For example, Han et al.[22] developed a deep learning-enhanced high-sensitivity VFA (hs-VFA) that leverages nanoparticle amplification and time-lapse imaging. This system achieved a detection limit of 0.2 pg/mL for cTnI, meeting clinical guidelines for high-sensitivity assays. The hs-VFA operates efficiently using 50 μL of serum and provides results within 15 min, supported by a portable Raspberry Pi-based reader. Computational enhancements, including outlier analysis and neural network-based quantification, further improved the precision of the system (CV < 7%) and extended its dynamic range to cover cTnI concentrations by over 6 orders of magnitude. In blinded testing with clinical samples, hs-VFA exhibited a strong correlation (Pearson's r of 0.965) with Food and Drug Administration (FDA)-approved benchtop analyzers.

Another study by the same research group introduced a chemiluminescence-based VFA (CL-VFA) platform for high-sensitivity cTnI detection.[100] This system incorporates a polymerized enzyme-based conjugate to enhance signal intensity, a tray-based VFA cartridge to streamline assays in stacked paper structures and ensure stable CL imaging, and a neural network-driven computational pipeline for the accurate classification and quantification of cTnI levels. The CL-VFA measures cTnI from 50 μL of serum sample within 25 min, achieving a detection limit of 0.16 pg/mL with high reproducibility (average CV < 15%).

To address the need for accessible and accurate hsCRP testing, Ballard et al.[20] demonstrated computationally enhanced VF-μPADs capable of achieving laboratory-grade

https://doi.org/10.1021/acssensors.5c00668
ACS Sens. 2025, 10, 3317−3339

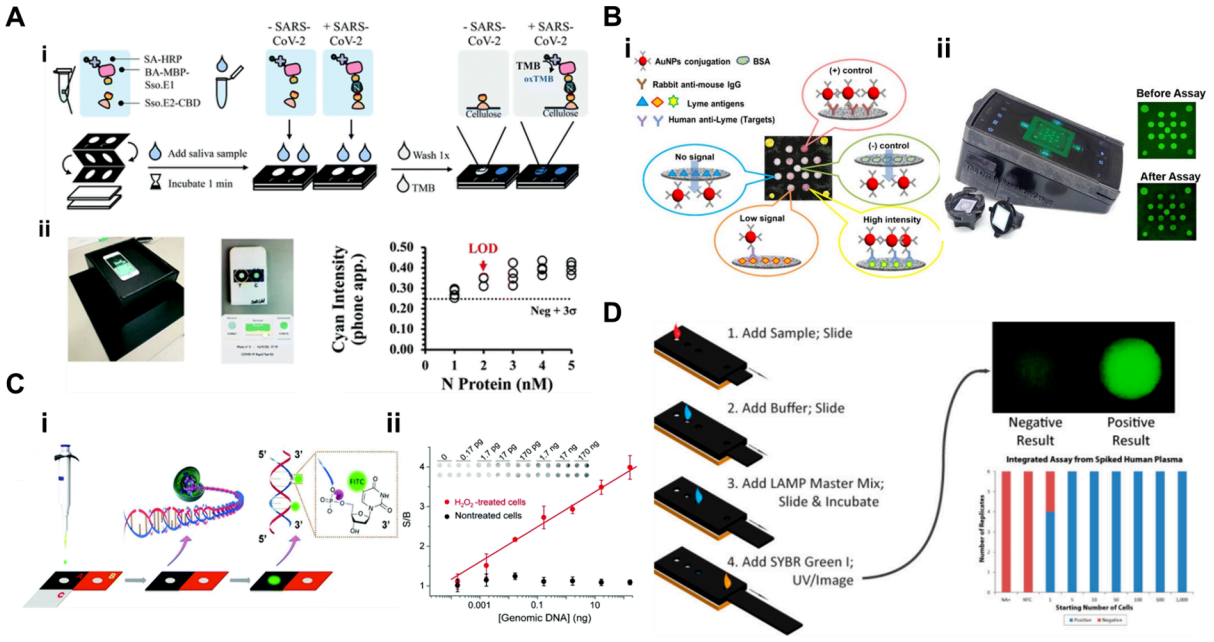

Figure 6. Applications of VF-μPADs for infectious diseases. (A) Smartphone-compatible VF-μPADs for rapid SARSCoV-2 antigen detection: (i) Assay workflow illustrating the VF-μPADs setup for SARS-CoV-2 antigen detection and (ii) device validation and calibration data with images of a light-controlled box and smartphone interface for real-time result analysis.[74] Reproduced with permission from ref (74). Copyright 2022 Royal Society of Chemistry. (B) Multiplexed VF-μPADs for the early detection of Lyme disease (LD): (i) illustration of the multiplexed immunoreactions that occur on the sensing membrane during the xVFA operation and (ii) photograph of the mobile-phone reader with an opened xVFA cassette and example images of the sensing membrane.[24] Reproduced with permission from ref (24). Copyright 2020 American Chemical Society. (C) DNA extraction and damage detection using an origami μPAD: (i) schematic of the assay workflow showing the DNA extraction integrated with TUNEL reaction on paper, creating a streamlined approach to DNA damage analysis and (ii) time-dependent S/B values showing that the paper-based TUNEL exhibited a significantly faster reaction rate constant (k^{paper} = 1.12 min^{-1}) compared to the solution-based TUNEL ($k^{solution}$ = 0.25 min^{-1}). To demonstrate its practical application, genomic DNA with and without H_2O_2 treatment was mixed with TUNEL reagents and applied to the paper chip.[85] Reproduced with permission from ref (85). Copyright 2021 Royal Society of Chemistry. (D) Slidingstrip loop-mediated isothermal amplification (LAMP) device for rapid and sensitive molecular diagnostics: Schematic of the LAMP device showing the sequential addition of sample, buffer, and reagents and sensitivity results.[63] Reproduced with permission from ref (63). Copyright 2015 American Chemical Society.

precision in POC settings. The hsCRP test holds clinical importance in stratifying CVD risk into low (<1 mg/L), intermediate (1−3 mg/L), and high (>3 mg/L) categories. This platform integrates a machine-learning-driven framework for optimizing the immunoreaction spot layout and signal quantification, utilizing a custom-designed mobile phone reader for portability and cost-effectiveness. The study featured a multiplexed sensing membrane with 81 spatially isolated immunoreaction spots optimized using neural networks. Blind testing with 85 clinical samples exhibited an R^2 of 0.95 and a CV of 11.2% across the hsCRP range (0−10 mg/L), meeting the FDA-recommended performance criteria. Notably, the computational VF-μPADs overcame hook-effect-induced inaccuracies by leveraging multiplexed channels with various conditions of antigen/antibody concentrations. Thus, this approach enhanced the dynamic range and reduced the risk of false positives, particularly at elevated CRP concentrations indicative of acute inflammation.

Protein Biomarkers for Infectious Diseases. During infectious disease outbreaks, antigen rapid tests (ARTs) enable healthcare workers to quickly identify infected individuals and implement appropriate public health measures. During the COVID-19 pandemic, lateral flow assays (LFAs) and antigen rapid tests (ARTs) were extensively used to address the diagnostic needs for widespread testing of SARS-CoV-2, influenza, and other illnesses. VF-μPADs can be utilized to develop diagnostic tests for infectious diseases, enabling faster and more accurate detection through their optimized fluid dynamics, enhanced multiplexing capabilities, and shorter assay times. These advantages, combined with the ability to design multiple biomarker panels, make VF-μPADs a promising platform for addressing future diagnostic challenges in resource-limited settings and high-demand scenarios.

For example, available LFA format ARTs rely heavily on NC membranes, which resulted in supply shortages during the COVID-19 pandemic.[74] VF-μPADs with cellulose paper as a test material provide a complementary test approach. For instance, Jia et al.[74] developed a smartphone-compatible VF-μPAD for SARS-CoV-2 N protein detection employing a cellulose pull-down test format, enabling one-step sample application and result readout from the same surface (Figure 6Ai and 6Aii). The VF-μPAD setup for SARS-CoV-2 antigen detection delivers rapid, on-site results within 3 min, making it ideal for high-demand screening (Figure 6Ai). This device is based on colorimetric detection and utilize a tetramethylbenzidine (TMB) substrate with horseradish peroxidase (HRP) to produce a cyan color signal, which is analyzed via smartphone imaging or spectrophotometry. It achieves a detection limit of 2.5 nM for SARS-CoV-2 N protein in laboratory settings and 6.3×10^4 $TCID_{50}$/mL for live virus detection. Validation and calibration images, including a light-controlled box and smartphone interface for real-time analysis, further demonstrate the VF-μPAD's versatility in POCT and its effectiveness in SARS-CoV-2 surveillance (Figure 6Aii).[74]

https://doi.org/10.1021/acssensors.5c00668
ACS Sens. 2025, 10, 3317−3339

Unlike antigen detection, diagnosing a specific disease through antibody detection, known as serology, often requires the simultaneous detection of multiple antibodies. This approach is essential to accurately assess the host immune response to various immunodominant epitopes associated with an infection. Since VF-μPADs offer distinct advantages for multiplexing, this capability is particularly valuable in infectious disease diagnostics, where it may be necessary to measure antibodies targeting various antigens that elicit an immune response. For example, Eryilmaz et al.[13] developed multiplexed VF-μPADs to detect IgG and IgM antibodies against five SARS-CoV-2 structural proteins: nucleocapsid (N), spike receptor-binding domain (RBD), spike subunit 1 (S1), spike subunit 2 (S2), and the membrane protein (M). This multiplexed test utilized a machine learning-based neural network to classify an individual's immunity status into three categories: protected, unprotected, or infected. The assay demonstrated an overall classification accuracy of 89.5%, requiring only 40 μL of serum and providing results in under 20 min. The study highlights the potential of VF-μPADs for community-wide screening and immune monitoring by offering rapid, cost-effective, and scalable testing for POC applications, enabling real-time insights into immunity and infection dynamics within populations.

Joung et al.[24] developed a VF-μPAD for the early detection of Lyme disease (LD), a prevalent zoonotic infection transmitted through the bite of Ixodes ticks. LD diagnosis often requires simultaneous analysis of multiple antibodies because early immune responses are varied and involve multiple antigens, such as OspC, BmpA, P41, DbpB, and Crasp1.[24] The antigen−antibody interactions occur within spatially separated immunoreaction spots on the VF-μPADs, enabling the parallel detection of multiple targets within a compact design (Figure 6Bi).[24] This device employs a colorimetric detection method, where gold nanoparticles conjugated with antihuman IgM or IgG antibodies bind to the target antibodies in serum samples. This interaction generates a visible color signal, with intensity proportional to the antibody concentration. The assay used a smartphone-compatible reader and neural network for automated diagnosis, achieving an area under the curve (AUC) of 0.950, with a sensitivity of 90.5% and a specificity of 87.0% during blind testing (Figure 6Bii).[24] After batch-specific standardization and threshold tuning, specificity increased to 96.3%. The entire assay was completed within 15 min, highlighting its potential use in POC diagnostics.

Recently, utilizing the same VF-μPAD platform, Ghosh et al.[23] advanced the diagnostic capabilities for LD by incorporating synthetic peptides as antigen mimics on the sensing membrane to specifically target various IgM and IgG antibodies. Nine unique peptides were multiplexed in duplicate within a single panel, creating 18 individual immunoreaction spots immobilized with synthetic peptides. Combined with positive and negative control spots, the assay included 25 distinct reaction spots. The unique flow-through design of VF-μPADs enables higher multiplexing detection using small peptide-based capture probes without compromising assay performance. This format prevents issues such as the wash-away of immobilized reagents or displacement of test lines, which can occur with capillary transport in traditional immunochemistry reactions. The use of peptide-based targets also improves the manufacturability of the VF-μPADs because synthetic peptides offer exceptional cost-effectiveness and scalability, as they are chemically synthesized and do not require the extensive purification processes needed for recombinant antigens. Furthermore, peptides provide improved stability, given that they do not depend on maintaining a native 3D conformation, ensuring a longer shelf life of the diagnostic test. This eliminates the need for cold chain storage conditions, which is a limitation in distribution, specifically in resource-limited or high-demand settings, such as a pandemic. The use of synthetic peptide targets enhances diagnostic accuracy by increasing sensitivity to target analytes while minimizing nonspecific protein−protein interactions, which is a common challenge in tests for emerging infections. By leveraging distinct peptides and a machine learning-based diagnostic algorithm, this study achieved 95% sensitivity and 100% specificity for LD detection in a single 20 min rapid test using serum samples. The peptide-based design eliminates cross-reactivity with potential look-alike diseases, significantly improving upon earlier iterations, achieving 87% specificity. These advancements underscore the transformative potential of peptide-based VF-μPADs for rapid, reliable, and scalable diagnostics, especially in addressing complex immune challenges.

Beyond LD diagnostics, VF-μPADs exemplify a broader trend toward the convergence of peptide-based antibody repertoire screening and rapid testing. Peptide microarrays have proven invaluable for epitope mapping and rapid antibody profiling, enabling the high-throughput analysis of immune responses.[101,102] The combination of VF-μPADs' rapid assay time and scalability of peptide-based diagnostics offers a unique convergence of technology, facilitating cost-effective, large-scale immune profiling. This approach not only enhances diagnostic performance but also aligns with the increasing demand for POC systems capable of addressing the complexities of immune system interactions with pathogens.

Nucleic Acid Detection. Beyond multiplexing, VF-μPADs excel in performing complex, multistep assays that are challenging for simpler paper-based devices. This design is particularly suited for assays that require multiple reaction steps, such as nucleic acid extraction[85] and amplification,[63] where precise control is essential. For example, Xue et al.[85] developed a VF-μPAD for DNA damage detection by integrating on-paper DNA extraction with the terminal deoxynucleotidyl transferase dUTP nick end labeling (TUNEL) reaction, a widely used assay for detecting apoptotic programmed cell death. This integration enables high-throughput, rapid genotoxicity testing, demonstrating the device's capability to handle complex assays efficiently (Figure 6Ci and 6Cii).[85] This device incorporates multiple functional layers to perform sequential operations, including cell lysis, DNA extraction, and a TUNEL reaction, followed by fluorescence-based signal detection. The foldable design facilitates precise fluid diffusion between the layers, thereby streamlining the assay process. (Figure 6Ci). Signal-to-background (S/B) values for paper-based TUNEL assays, compared to solution-based assays, demonstrate improved efficiency on the VF-μPADs (Figure 6Cii). This method enables rapid and sensitive DNA damage detection, completing DNA extraction in 7 min and the entire assay within 30 min. The device achieves a detection limit of 1.7 pg of DNA and is capable of detecting DNA damage in as few as 10 cells, demonstrating high sensitivity. Additionally, the TUNEL reaction on paper shows a significantly higher reaction rate (k^{paper} = 1.12 min^{-1}) compared to solution-based assays

https://doi.org/10.1021/acssensors.5c00668
ACS Sens. 2025, 10, 3317−3339

Table 2. VF-μPADs for in Vitro Diagnostics

Target analyte(s)	Fabrication method	Used materials	Sensing modality	Specimen (volume, μL)	Detection limit	Ref.
Small molecules: Iron	Stacking	Cellulose membrane, glass fiber, and polysulfone	Colorimetric	Whole blood (50 μL)	Spiked sample:0.0004.AU μg^{-1} dL^{-1}	56
Small molecules: Glucose, BSA	Stacking	Cellulose membrane	Colorimetric	PBS (80 μL)	Buffer-based: 0.7 mM (glucose), 18 mM (BSA)	95
Small molecules: Glucose, Lactate	Stacking	Cellulose membrane	Colorimetric	PBS (15 μL)	Buffer-based: 0.3 mM (glucose), 0.02 mM (lactate)	96
Small molecules: Methyl parathion	Origami/folding	Cellulose membrane	Potentiometric	10 μL	Spiked sample: 0.06 nM	87
Small molecules: Cyanide ion	Origami/folding	Cellulose membrane	Colorimetric	Borate buffer (2 μL)	Buffer-based: 0.4 μmol/L	88
Small molecules: Mercury, Glucose	Origami/folding	Cellulose membrane	Electrochemical	Tap water (mercury, 10 μL), Sweat (glucose, 10 μL)	NA	90
Small molecules: Glucose, Cholesterol, Albumin, ALP, Creatinine, AST, ALT, Urea Nitrogen	3D printing	Cellulose membrane	Colorimetric	NA	Buffer-based: 0.3 mmol/L (glucose), 0.3 mmol/L (cholesterol), 0.1 g/dL (albumin), 10 U/L (ALP), 40 μmol/L (creatinine), 10 U/L (AST), 50 U/L (ALT), 0.04 mmol/L (Urea Nitrogen)	38
Small molecules: Glucose	3D printing	Cellulose membrane, and Polysulfone	Colorimetric	Whole blood (100 μL)	Spiked sample: 0.3 mM	18
Small molecules: Dopamine	3D printing	Cellulose membrane	Fluorescence	Tris-buffer (59 μL)	NA	99
Small molecules: Glucose, Albumin	3D printing	Cellulose membrane	Colorimetric	Artificial urine (5 μL)	Buffer-based: 0.8 mM (glucose), 3.5 μM (albumin)	15
Protein-noninfectious disease: Myoglobin, creatine kinase-MB (CK-MB), and heart-type fatty acid binding protein (h-FABP)	Stacking	NC membrane, Polysulfone, and cotton fiber	Fluorescence	Serum (50 μL)	Spiked sample: 0.52 ng/mL (Myoglobin), 0.3 ng/mL (CK-MB), 0.49 ng/mL (h-FABP)	21
Protein-noninfectious disease: Cardiac troponin I (cTnI)	Stacking	NC membrane, Polysulfone, and cotton fiber	Colorimetric	Serum (50 μL)	Spiked sample: 0.2 pg/mL	22
Protein-noninfectious disease: Cardiac troponin I (cTnI)	Stacking	NC membrane, Polysulfone, and cotton fiber	Chemiluminescence	Serum (50 μL)	Spiked sample: 0.16 pg/mL	100
Protein-noninfectious disease: Alkaline phosphatase, β-d-galactosidase	Stacking	Cellulose membrane	Colorimetric	Serum	Spiked sample: 2.4 pM (alkaline phosphatase)	93
Protein-noninfectious disease: Blood alanine aminotransferase (ALT)	Stacking	Plasma separation membrane	Colorimetric	Whole blood (40 μL)	Spiked sample: 53 U/L	57
Protein-noninfectious disease: C-reactive protein (CRP)	Stacking	Cellulose membrane, NC membrane	Colorimetric	Whole blood (100 μL)	Spiked sample: 40 ng/mL	94
Protein-noninfectious disease: Ammonia, Carbon dioxide, Urea	Origami/folding	Cellulose membrane	Colorimetric	Saliva/plasma (2 μL)	Spiked sample: 0.03 mg/dL (ammonia), 0.06 mg/dL (carbon dioxide), 0.18 mg/dL (urea)	86
Protein-noninfectious disease: Human serum albumin (HSA), Human immunoglobulin G (HIgG)	Origami/folding	Cellulose membrane	Electrochemical	Priming buffer (20 μL)	Buffer-based: 1.5 pM	89
Protein-infectious disease: IgM/IgG antibodies for Lyme disease	Stacking	NC membrane, Polysulfone, and cotton fiber	Colorimetric	Serum (50 μL)	Buffer-based:209.6 ng/mL (anti-OspC), 162.2 ng/mL (anti-BmpA), 1.05 μg/mL (anti-P41)	12
Protein-infectious disease: IgM/IgG antibodies for SARS-CoV-2	Stacking	NC membrane, Polysulfone, and cotton fiber	Colorimetric	Serum (40 μL; 20 μL each for IgM and IgG tests)	Undetermined	13
Protein-infectious disease: IgM/IgG antibodies for Lyme disease	Stacking	NC membrane, Polysulfone, and cotton fiber	Colorimetric	Serum (20 μL)	Undetermined	23
Protein-infectious disease: H1N1 virus	Stacking	Cellulose membrane, Polytetrafluorethylene membrane	Electrochemical, Colorimetric	Saliva (40 μL)	Spike sample: 4.7 PFU/mL by electrochemical method, 2.27 PFU/mL by colorimetric method	97
Protein-infectious disease: Human norovirus	Stacking	Cellulose/polyester paper, NC membrane	Colorimetric	PBS (110 μL)	Buffer-based: 9.5 × 104 copies/mL	98
Protein-infectious disease: Protein A for *S. aureus*	Origami/folding	Cellulose membrane	Colorimetric	Real sample: Synovial fluid (3 μL)	NA	48
Protein-infectious disease: Dengue virus serotypes	3D printing	Cellulose membrane	Colorimetric	45 μL	Buffer-based: 23.28 nM (DENV-1), 5.23 nM (DENV-2), 38.17 nM (DENV-3), and 29.64 nM (DENV-4)	80
Nucleic acid: Hepatitis B Virus DNA	Origami/folding	Cellulose membrane	Electrochemical	Trailing electrolyte solution (50 μL)	NA	61

https://doi.org/10.1021/acssensors.5c00668
ACS Sens. 2025, 10, 3317−3339

Table 2. continued

Target analyte(s)	Fabrication method	Used materials	Sensing modality	Specimen (volume, μL)	Detection limit	Ref.
Nucleic acid: SARS-CoV-2 RNA and its variants	Origami/ folding	Cellulose membrane	Colorimetric	Molecular biology grade H_2O (5 μL)	Buffer-based: 400 copies/μL (SARS-CoV-2 RNA)	91
Nucleic acid: *E. coli* O157: H7, Salmonella	Origami/ folding	Cellulose membrane	Colorimetric	25 μL (bacterial solution), 15 μL (LAMP reaction)	Buffer-based: 25 CFU	92

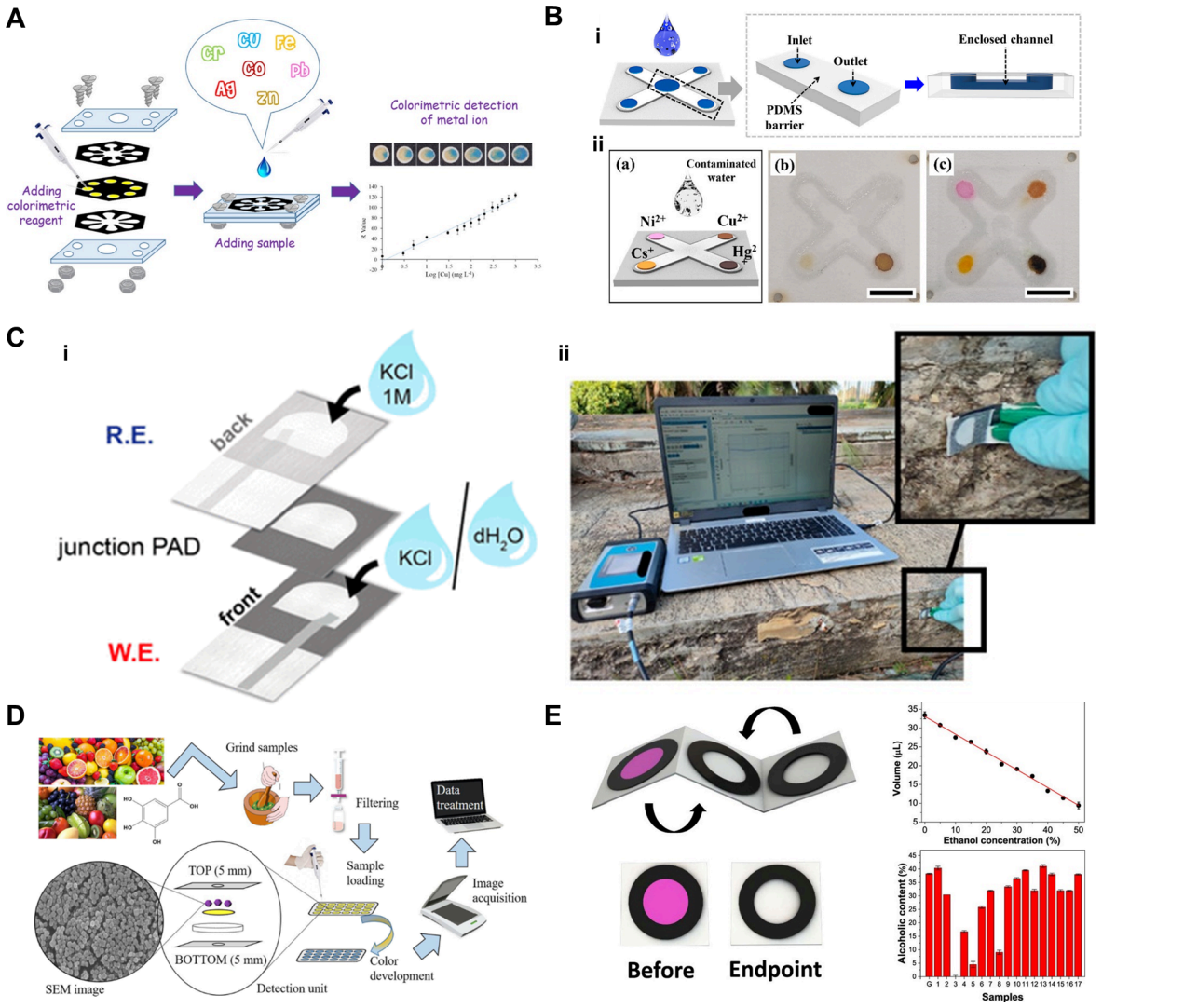

Figure 7. Application of VF-μPADs for environmental monitoring and agriculture. (A) VF-μPAD design with a functional waste reservoir layer, enabling increased sample volume capacity for colorimetric assay of heavy metal ions.[103] Reproduced with permission from ref (103). Copyright 2020 Elsevier B.V. (B) Enclosed VF-μPADs for the simultaneous detection of heavy metal ions and a radioactive isotope in water environment. (i) Schematic illustration of enclosed VF-μPADs with four channels for multiplex detection. (ii) (a, b) Multiplex colorimetric response for detection of water samples contaminated with nickel (Ni^{2+}), copper (Cu^{2+}), mercury (Hg^{2+}), and cesium (Cs^{+}) ions.[104] Reproduced with permission from ref (104). Available under a CC-BY license. Copyright 2023 MDPI. (C) Sensor integrated VF-μPADs for on-site and prompt evaluation of chloride contamination in concrete structures. (i) Design of the vertical flow paper-based sensor. The device is loaded with a few microliters of two solutions having different concentrations of chlorides, drop-cast on the top layer and on the bottom layer. (ii) Photos of the experimental setup applied to concrete. (iii) Chloride evaluation: a portion of the building fundament, a wall from the basement, and the monumental stairs.[105] Reproduced with permission from ref (105). Copyright 2021 American Chemical Society. (D) VF-μPADs combined with metal−organic frameworks in a single device for phenolic content assessment in fruits.[106] Reproduced with permission from ref (106). Available under a CC-BY license. Copyright 2023 Springer Nature. (E) VF-μPADs for the visual determination of alcohol content in whiskey samples. (i) Layout of the foldable VF-μPADs and the test spots for before and end point of detection (ii) Calibration curve for ethanol and alcoholic content determined for seized samples using a foldable VF-μPADs.[108] Reproduced with permission from ref (108). Copyright 2018 Elsevier B.V.

($k^{solution}$ = 0.25 min^{-1}), attributed to the localized concentration of DNA and reagents on the paper substrate. By integrating on-paper nucleic acid extraction and analysis, this VF-μPAD exemplifies the versatility and efficiency of paper-based platforms for nucleic acid detection in diverse applications.

https://doi.org/10.1021/acssensors.5c00668
ACS Sens. 2025, 10, 3317−3339

Additionally, a sliding-strip paper device for molecular diagnostics integrates sample preparation with loop-mediated isothermal amplification (LAMP) for *Escherichia coli* DNA detection and streamline multistep workflows into a portable testing format. This approach simplifies complex assays, making it suitable for on-site diagnostics (Figure 6Di).[63] This device incorporates stepwise sample, buffer, and reagent addition through designated channels, with each channel assigned to specific tasks such as preparation, extraction, amplification, and readout, thus reducing the need for pipetting. Detection is based on a fluorescence-based readout utilizing SYBR Green I, a fluorescent intercalating dye that is excited by a hand-held UV source and imaged using a smartphone camera. The analytical sensitivity demonstrated the ability to detect as few as one double-stranded DNA target copy, highlighting its exceptional sensitivity. When testing live *E. coli* spiked into human plasma, the device reliably detected as few as five cells and successfully detected even a single cell in 67% of cases. Analytical sensitivity results highlight its ability for highly sensitive DNA detection, making it especially valuable in low-resource settings where precision and minimal sample handling are critical (Figure 6Dii).[63] This study highlights the unique ability of VF-μPADs to integrate complex workflows and achieve high sensitivity in DNA detection, providing a valuable tool for molecular diagnostics in diverse applications. Table 2 summarizes the applications of VF-μPADs for in vitro diagnostics.[12,13,15,18,21−23,38,48,56,57,61,80,86−100]

ENVIRONMENTAL MONITORING AND AGRICULTURE

Environmental monitoring and agriculture often require the detection of multiple markers in real samples, making VF-μPADs more advantageous than LF-μPADs due to their superior flow control and multiplexing capabilities. VF-μPADs have demonstrated their versatility in detecting a wide range of analytes relevant to environmental monitoring and agriculture, including heavy metals,[103,104] chloride ions,[105] phenolic compounds,[106,107] alcohol[108] etc. These analytes are critical for assessing environmental health, water safety, and quality of agricultural products.

Environmental Monitoring. Heavy metals are commonly detected using μPADs because of their environmental impact and associated health risks. However, heavy metal ions with high charge density interact strongly with the carboxyl groups of the paper membrane, limiting their ability to travel long distances.[103] Consequently, VF-μPADs, which feature relatively shorter fluidic paths, offer distinct advantages for heavy metal detection. Sharifi et al.[103] developed VF-μPADs with a polyvinyl chloride (PVC) membrane for detecting heavy metal ions, specifically Cu^{2+}, in water samples (Figure 7A). The vertical flow mechanism enabled the sample to pass through stacked paper layers, where the PVC membrane immobilized the colorimetric reagents, effectively preventing dye leaching and ensuring uniform color distribution. To further optimize this process, an additional functional layer acting as a waste reservoir was incorporated. This layer effectively managed the excess sample solution, prevented overflow, and facilitated the transport of additional analytes to the detection zone. The structural advantages of VF-μPADs increased the device's sample volume capacity, enhanced the colorimetric signal intensity by approximately 2.5 times, and enabled the detection of Cu^{2+} at concentrations as low as 30 mg/L in both rainwater and tap water.[103] Furthermore, their stacking design not only contributes to sample volume capacity but also offers significant advantages in preventing sample evaporation and contamination.[104] Choi et al.[104] developed an enclosed VF-μPADs for the simultaneous detection of heavy metal ions (Cu^{2+}, Ni^{2+}, and Hg^{2+}) and a radioactive isotope (Cs^{+}) in water samples (Figure 7B). The sample traveled vertically and laterally through hydrophilic channels surrounded by PDMS barriers, thereby enhancing fluid control, preventing evaporation, and minimizing contamination. The device demonstrated rapid colorimetric detection within 3 min for a concentration range of 0.1−2000 ppm, with a detection limit of 0.55 ppm for Ni^{2+}, 5.05 ppm for Cu^{2+}, 0.188 ppm for Hg^{2+}, and 0.016 ppm for Cs^{+}, ensuring reliable qualitative and quantitative analysis. This enclosed design prevents sample loss and ensures consistent results, thereby enhancing its potential as a primary early detection tool for ionic contaminants in various applications.[104]

The corrosion of reinforced concrete has emerged as a significant concern in the modern era, given its status as the most widely used material in the construction industry. Among the numerous factors contributing to the degradation of metallic reinforcements, the ingress of chloride ions into a concrete matrix poses one of the most severe threats. Chloride ions expedite the corrosion processes, progressively undermining the structural integrity of concrete over time. Colozza et al.[105] introduced vertical-flow potentiometric PADs designed to measure the electrochemical potentials of two solutions with differing chloride ion concentrations (Figure 7C). The device was designed to enable diffusion through the vertically stacked layers by introducing two solutions with different chloride concentrations into the top and bottom layers. This vertical stacking mechanism facilitates the measurement of the potential difference between the reference and working layers, enabling the detection of chloride ion concentrations. This approach allows for the straightforward and rapid detection of chloride ions without requiring complex instrumentation, making it especially useful for real-time, on-site monitoring.[105]

Agriculture. Phenolic compounds contribute to health benefits in fruits and therefore are critical for evaluating their nutritional and antioxidant properties. Their antioxidant activity aids in disease prevention and their concentration serves as a key indicator of fruit quality, ripeness, and shelf life. Cost-effective detection of these compounds is vital for food safety and quality control, making μPADs an ideal choice because of their affordability, simplicity, and portability. VF-μPADs enable rapid, on-site testing with minimal sample preparation and reagent use, offering both practicality and environmental sustainability. This combination of advantages ensures the efficient monitoring of phenolic content in fruits for health-related and market-value purposes. For example, Martinez et al.[106] utilized VF-μPADs combined with ZIF-8, a metal−organic framework (MOF), to detect and quantify phenolic content in fruit samples (Figure 7D). The device employs vertical flow, in which liquid samples traverse layers of filter paper, facilitating efficient sample processing and interaction with detection zones. ZIF-8, composed of zinc ions coordinated with 2-methylimidazole, was integrated into paper layers to enhance the retention and capture of phenolic compounds. Its high surface area, porous structure, and selective adsorption properties allow for strong binding with phenolic compounds, improving detection sensitivity and

https://doi.org/10.1021/acssensors.5c00668
ACS Sens. 2025, 10, 3317−3339

Table 3. VF-μPADs for Environmental Monitoring and Agriculture

Specimen (volume, μL)	Fabrication method	Used materials	Sensing modality	Target analyte(s)	Detection limit	Ref.
Rainwater, Tap water (40 μL)	Stacking	Cellulose membrane	Colorimetric	Cu^{2+}	Buffer-based: 1.7 mg/L	103
Groundwater, Stream water, (50 μL)	Stacking	Cellulose membrane	Electrochemical, Colorimetric	Pb^{2+}, Cd^{2+}, Cu^{2+}	Buffer-based: 0.1 ng/L (Pb^{2+}), 0.1 ng/L (Cd^{2+}), 4.12 ng/L (Cu^{2+})	110
Contaminated water (NA)	Stacking	Cellulose membrane	Colorimetric	Ni^{2+}, Cu^{2+}, Hg^{2+}, Cs^{+}	Buffer-based: 0.55 ppm (Ni^{2+}), 5.05 ppm (Cu^{2+}), 0.188 ppm (Hg^{2+}), 0.016 ppm (Cs^{+})	104
Drinking water, River water, Soil (3 μL)	Stacking	Cellulose membrane	Colorimetric	Hg^{2+}	Buffer-based: 20 mg/L	112
Tap water, lake water (130 μL)	Stacking	Cellulose membrane	Colorimetric	Fe^{3+}, Ni^{2+}, Cr^{4+}, Cu^{2+}, Al^{3+}, and Zn^{2+}	Buffer-based: 0.2 mg/L (Fe^{3+}), 0.3 mg/L (Ni^{2+}), 0.1 mg/L (Cr^{4+}), 0.03 mg/L (Cu^{2+}), 0.08 mg/L (Al^{3+}), 0.04 mg/L (Zn^{2+})	113
Lake water, Seawater (30 μL)	Stacking	Cellulose membrane	Colorimetric	Cd^{2+}, Pb^{2+}	Buffer-based: 0.245 μg/L (Cd^{2+}), 0.335 μg/L (Pb^{2+})	114
Coastal water, Seawater (40 μL)	Stacking	Cellulose membrane	Colorimetric	Cu^{2+}, Cd^{2+}, Pb^{2+}, Hg^{2+}	Buffer-based: 0.25 μg/L (Cu^{2+}), 0.17 μg/L (Cd^{2+}), 0.23 μg/L (Pb^{2+}), 0.36 μg/L (Hg^{2+})	115
PBS (3 μL)	Stacking	Cellulose membrane	Colorimetric	Pesticide	Buffer-based: 8.60 ppm	116
Tap water, Bottled water (2.5 mL)	Stacking	Cellulose membrane	Colorimetric	Hg^{2+}	Buffer-based: 1.2 nM	117
River water (5 μL)	Origami/ folding	Cellulose membrane	Electrochemical	Pesticide (paraoxon)	Buffer-based: 2 ppb (paraoxon)	120
Drinking water, River water (400 μL)	Origami/ folding	Cellulose membrane	Colorimetric	Ni^{2+}, Cu^{2+}, Fe^{3+}	Buffer-based: 2 ppm (Ni^{2+}), 0.3 ppm (Cu^{2+}), 1.1 ppm (Fe^{3+})	122
Liquid DMMP (20 μL)	Origami/ folding	Cellulose membrane	Colorimetric	Dimethyl methylphosphonate (DMMP)	Semiquantitative	123
H2O, Concrete (10 μL)	Stacking	Cellulose membrane	Electrochemical	Chlorides	Buffer-based: 5×10^{-2} M	105
Airborne particulate matter (PM) from Fuzhou City, China (0.3 μL)	Stacking	Cellulose membrane	Colorimetric	Fe, Cu, Ni	Buffer-based: 16.6 ng (Fe), 5.1 ng (Cu), 9.9 ng (Ni)	119
Apple, Cucumber, Tomato (15 μL)	Stacking	Cellulose membrane	Colorimetric	Malathion (insecticide)	Buffer-based: 6 nmol/L	111
Fruit samples (50 μL)	Stacking	Cellulose membrane	Colorimetric	Phenolic compounds	Buffer-based: 0.5 mg/L	106
Wine samples (25 μL)	Stacking	Cellulose membrane	Colorimetric	Phenolic compounds	Buffer-based: 1.2 mg/L	107
Brassica pekinensis, Brassica chinensis (12 μL)	Stacking	Cellulose membrane	Colorimetric	Pesticides (profenofo, methomyl)	Buffer-based: 55 nM (profenofo), 34 nM (methomyl)	118
Whiskey samples (1 μL)	Origami/ folding	Cellulose membrane	Colorimetric	Alcohol	Buffer-based: 2.10%	108
Seaweeds (35 μL)	Origami/ folding	Cellulose membrane	Colorimetric	Iodine (I^{-}, IO^{3-})	Buffer-based: 9.8 μM (I^{-}), 0.6 μM (IO^{3-})	121

accuracy.[106] Similarly, VF-μPADs have been employed to measure total phenolic compounds in wine.[107] High-performance liquid chromatography (HPLC), a common method for phenolic analysis, requires expensive instrumentation and maintenance, with initial setup costs ranging from $10,000 to over $50,000, excluding operational expenses.[109] In contrast, VF-μPADs offer a more affordable alternative, with production costs below 50 cents per unit, making them particularly suitable for rapid and environmentally friendly in-field applications.

VF-μPADs, with distinct functional layers designed for specific roles, can be utilized for alcohol content determination based on redox titration.[108] The device developed by Nogueira et al.[108] features a foldable, paper-based structure with three distinct functional layers: detection, reaction, and titrant addition (Figure 7E). The vertical flow mechanism enables the sample to traverse these layers, facilitating the oxidation of ethanol by potassium permanganate in an acidic medium. This reaction produces a color change that visually indicates the titration end point, thereby offering a straightforward and effective method for on-site analysis. The VF-μPADs stand out for their portability, affordability, and rapid analysis time of under 1 min. Requiring only a minimal sample volume (1 μL), they produce negligible waste and eliminate the need for complex instrumentation. These characteristics make these devices ideal for the forensic screening of whiskey samples, particularly for the quick and efficient detection of adulterated alcohol.[108] Table 3 summarizes the applications of VF-μPADs for environmental monitoring and agriculture.[110−123]

CHALLENGES AND FUTURE DIRECTIONS

While VF-μPADs offer significant advantages over traditional μPADs, several challenges must be addressed to harness their full potential. A key obstacle lies in the complexity of integrating multiple functional layers—such as sensing membranes, conjugation pads, and flow-control membranes—within a single device. These layers require intricate patterning and assembly. These production challenges can be overcome by reducing costs and enhancing scalability. This can be realized by transitioning from prototyping techniques, such as 3D printing, to scalable methods, such as injection molding for casings, and adopting mass-manufacturing tools akin to

https://doi.org/10.1021/acssensors.5c00668
ACS Sens. 2025, 10, 3317−3339

those used in lateral flow assays. For instance, laser cutting can streamline membrane patterning, whereas removing unnecessary layers or optimizing the device design for manufacturability can simplify production. Standardizing fabrication processes and developing automated production methods are critical for commercial viability.

Multiplexed detection, which allows simultaneous analysis of multiple biomarkers, is another promising feature of VF-μPADs. However, interpretation of these complex results remains challenging. Future devices should incorporate digital readers or smartphone-based tools to process the detection spots and provide diagnostic insights. Emerging technologies such as machine learning and automated digital readouts can simplify result interpretation, making these devices more accessible to users with limited technical expertise.

Material innovations and sensor integration offer additional pathways for enhancing VF-μPADs performance. Nanomaterials, including fluorescence nanoparticles,[21] carbon nanoparticles,[66] and surface-enhanced Raman scattering nanotags,[124] hold great promise for improving assay sensitivity, particularly for detecting early stage diseases and challenging biomarkers with extremely low clinical cutoff concentrations. Moreover, the integration of electronic sensors for real-time monitoring can expand the functionality and reliability of VF-μPADs, making them suitable for a broader range of diagnostic applications. A notable example is recently developed paper-based analytical cartridge integrated with a field-effect transistor (FET) and deep learning-based kinetic analysis.[125] This approach enhances assay sensitivity by leveraging FET biosensors for real-time electrical measurements while eliminating the need for complex surface chemistry, thus ensuring cost-effective operation. The deep learning framework further improves analytical accuracy by mitigating sample matrix effects and optimizing kinetic data interpretation.

While VF-μPADs demonstrate promising analytical performance in controlled settings, their widespread adoption requires thorough analytical validation.[126] This typically involves assessing parameters such as accuracy, precision, limit of detection, linearity, and reproducibility by comparing results to those obtained with reference laboratory methods. Standard validation procedures include spike-and-recovery experiments, inter- and intra-assay variation studies, and calibration curve analysis using serial dilutions. However, such evaluations in paper-based systems are often challenged by matrix effects, nonuniform fluid flow, and variability across batches. Moreover, many reported VF-μPADs are tested only with model or spiked samples; validation using real patient specimens or environmental matrices such as whole blood, serum, plasma, urine, saliva, or river/seawater is essential, as these can introduce sample matrix-related issues like nonspecific binding and signal suppression. Addressing these challenges during the assay optimization and validation stage is critical to ensuring the clinical and practical reliability of VF-μPADs. For VF-μPADs validated with clinical or real-world samples, performance metrics such as Pearson's correlation coefficient, limit of detection, sensitivity, and specificity are commonly used to demonstrate the diagnostic utility of the platform in its intended application. These metrics are essential for translating laboratory-based devices into clinically relevant and field-deployable systems.

The integration of artificial intelligence (AI), deep learning (DL) and machine learning (ML) is increasingly recognized as a transformative direction for POC diagnostics, including VF-μPADs.[127] These computational tools are capable of automated signal recognition, processing complex data sets, enhancing signal interpretation, and enabling dynamic decision-making without human intervention. Convolutional neural networks (CNNs) and fully connected neural networks (FCNNs) have already been applied to VF-μPADs and imaging-based platforms to improve diagnostic accuracy, reduce false readings, and support quantification of biomarkers across diverse clinical conditions.[20−22] Moreover, AI-assisted optimization of assay design, such as selecting optimal immunoreaction spot configurations or adjusting reagent parameters, can significantly reduce development time and cost.[128] As POCT systems generate more data through frequent, decentralized use, AI-enabled models will become essential for real-time learning, predictive diagnostics, and personalized testing.[129,130] While challenges remain—including model interpretability, regulatory approval, and data privacy—the synergy between AI and POCT represents a crucial step toward the development of intelligent, scalable, and accessible diagnostics for global health applications.

To make VF-μPADs more user-friendly for at-home or decentralized use, automating sequential liquid handling steps is essential. Currently, the manual addition of reagents at specific intervals complicates the operation for nonexpert users. Incorporating passive, hands-free liquid handling mechanisms—such as soluble polymer-based fluidic valves,[131,132] similar to those explored in LFA systems—that automate multistep reactions can streamline workflows and enhance usability. In addition to reagent handling, end-users without technical expertise may struggle with issues such as inconsistent sample application, difficulty interpreting subtle colorimetric changes, and accidental contamination during device operation. These challenges can significantly affect the reliability of results in practical settings. Therefore, future VF-μPAD designs should prioritize user-centered features such as preloaded reagents, built-in color references, and mobile device-based readers to minimize operator-dependent variability. This advancement would bring VF-μPADs closer to realizing their full potential as robust and scalable diagnostic tools.

CONCLUSION

LF-μPADs continue to be a popular choice for simple and cost-effective diagnostics, particularly in resource-limited settings. Their lateral flow mechanism enables rapid and straightforward assays; however, it limits multiplexing capability and is susceptible to the hook effect at higher analyte concentrations, which can compromise sensitivity and accuracy. In contrast, VF-μPADs, with their vertical flow design and parallel immunoreaction zones, overcome these limitations by providing (1) multiplexing capability, (2) reduced hook effect, and (3) reduced sample-to-answer time. This vertical configuration improves fluid movement and sample interaction with detection reagents, enabling VF-μPADs to produce more consistent and reliable results.

VF-μPADs may provide cost-effective solutions for environmental monitoring and advanced diagnostics, particularly for POC applications and pandemic preparedness, where accuracy, scalability, and rapid results are essential. They are highly effective in detecting an array of analytes or contaminants. To build upon these strengths, future advancements should focus on scaling up fabrication methods, integrating advanced materials (i.e., new functional paper membrane or detection

https://doi.org/10.1021/acssensors.5c00668
ACS Sens. 2025, 10, 3317−3339

conjugate labels) to enhance sensitivity, and incorporating electronic sensors for real-time data analysis. These improvements will further expand the scope of VF-μPADs applications, making them adaptable for addressing public health and environmental challenges through timely, on-site assessments.

AUTHOR INFORMATION

Corresponding Authors

Aydogan Ozcan − *Department of Electrical & Computer Engineering, Department of Bioengineering, and California NanoSystems Institute (CNSI), University of California, Los Angeles, California 90095, United States;* orcid.org/0000-0002-0717-683X; Email: ozcan@ucla.edu

Sungsu Park − *School of Mechanical Engineering, Department of Biophysics, Institute of Quantum Biophysics (IQB), and Department of Metabiohealth, Sungkyunkwan University (SKKU), Suwon 16419, Korea;* orcid.org/0000-0003-3062-1302; Email: nanopark@skku.edu

Authors

Jaehyung Jeon − *School of Mechanical Engineering, Sungkyunkwan University (SKKU), Suwon 16419, Korea; Department of Electrical & Computer Engineering, University of California, Los Angeles, California 90095, United States*

Heeseon Choi − *School of Mechanical Engineering, Sungkyunkwan University (SKKU), Suwon 16419, Korea*

Gyeo-Re Han − *Department of Electrical & Computer Engineering, University of California, Los Angeles, California 90095, United States;* orcid.org/0000-0003-3584-4433

Rajesh Ghosh − *Department of Bioengineering, University of California, Los Angeles, California 90095, United States;* orcid.org/0000-0002-7408-8944

Barath Palanisamy − *Department of Bioengineering, University of California, Los Angeles, California 90095, United States;* orcid.org/0000-0002-7117-2876

Dino Di Carlo − *Department of Bioengineering and California NanoSystems Institute (CNSI), University of California, Los Angeles, California 90095, United States;* orcid.org/0000-0003-3942-4284

Complete contact information is available at: https://pubs.acs.org/10.1021/acssensors.5c00668

Author Contributions

Jaehyung Jeon: Writing−original draft and conceptualization, Writing - review and editing, Drawing figures. Heeseon Choi: Writing - review and editing, Drawing figures. Gyeo-Re Han, Rajesh Ghosh, Barath Palanisamy, Dino Di Carlo: Writing - review and editing. Sungsu Park: Writing−review and editing, Supervision, Project administration, Funding acquisition. Aydogan Ozcan: Writing− review and editing, Supervision, Project administration, Funding acquisition.

Notes

The authors declare no competing financial interest.

ACKNOWLEDGMENTS

This work was supported by the National Research Foundation of Korea (NRF) grant (No. RS-2023-00234581) and (No. 2023R1A2C2006310) funded by the Korean government (MSIT). J.J. was supported by a grant from the Korea Health Technology R&D Project through the Korea Health Industry Development Institute (KHIDI), funded by the Ministry of Health & Welfare, Republic of Korea (grant number: HI19C1348). D.D. and A.O. are supported by the U.S. National Science Foundation Awards 1648451, 2345816, and 2149551 and National Institutes of Health Awards R44AI184034 and R44AI150060.

VOCABULARY

Paper-based analytical devices: Low-cost diagnostic platforms that use paper as a substrate for chemical or biological analysis, leveraging capillary action to transport fluids without external pumps.

Vertical flow paper-based analytical devices: A paper-based diagnostic format in which fluids flow vertically through stacked porous layers, typically from top to bottom, enabling integration of separation and detection steps in layered structures.

In vitro diagnostics: Tests performed on biological samples such as blood, urine, or saliva outside the human body to detect diseases or monitor health conditions.

Environmental monitoring: The systematic sampling and analysis of environmental media—such as air, water, or food—to assess pollution levels, detect hazardous substances, or ensure regulatory compliance.

Multiplexing: The simultaneous detection or measurement of multiple analytes within a single test, increasing throughput and efficiency in diagnostic or sensing applications.

Point of care testing: Diagnostic testing conducted at or near the site of patient care, providing rapid results without the need for centralized laboratory infrastructure.

REFERENCES

(1) Vaitukaitis, J. L.; Braunstein, G. D.; Ross, G. T. A radioimmunoassay which specifically measures human chorionic gonadotropin in the presence of human luteinizing hormone. *Am. J. Obstet. Gynecol.* **1972**, *113* (6), 751−758.

(2) Nanthasurasak, P.; Cabot, J. M.; See, H. H.; Guijt, R. M.; Breadmore, M. C. Electrophoretic separations on paper: Past, present, and future-A review. *Anal. Chim. Acta* **2017**, *985*, 7−23.

(3) Gantelius, J.; Bass, T.; Sjöberg, R.; Nilsson, P.; Andersson-Svahn, H. A Lateral Flow Protein Microarray for Rapid and Sensitive Antibody Assays. *Int. J. Mol. Sci.* **2011**, *12* (11), 7748−7759.

(4) Mudanyali, O.; Dimitrov, S.; Sikora, U.; Padmanabhan, S.; Navruz, I.; Ozcan, A. Integrated rapid-diagnostic-test reader platform on a cellphone. *Lab Chip* **2012**, *12* (15), 2678−2686.

(5) Martinez, A. W.; Phillips, S. T.; Whitesides, G. M.; Carrilho, E. Diagnostics for the Developing World: Microfluidic Paper-Based Analytical Devices. *Anal. Chem.* **2010**, *82* (1), 3−10.

(6) Martinez, A. W.; Phillips, S. T.; Whitesides, G. M. Three-dimensional microfluidic devices fabricated in layered paper and tape. *Proc. Natl. Acad. Sci. U.S.A.* **2008**, *105* (50), 19606−19611.

(7) Oh, Y. K.; Joung, H. A.; Kim, S.; Kim, M. G. Vertical flow immunoassay (VFA) biosensor for a rapid one-step immunoassay. *Lab Chip* **2013**, *13* (5), 768−772.

(8) Amarasiri Fernando, S.; Wilson, G. S. Studies of the Hook Effect in the One-Step Sandwich Immunoassay. *J. Immunol. Methods* **1992**, *151* (1−2), 47−66.

(9) Clarke, O. J. R.; Goodall, B. L.; Hui, H. P.; Vats, N.; Brosseau, C. L. Development of a SERS-Based Rapid Vertical Flow Assay for Point-of Care Diagnostics. *Anal. Chem.* **2017**, *89* (3), 1405−1410.

(10) Chen, P.; Gates-Hollingsworth, M.; Pandit, S.; Park, A.; Montgomery, D.; AuCoin, D.; Gu, J.; Zenhausern, F. Paper-based Vertical Flow Immunoassay (VFI) for detection of bio-threat pathogens. *Talanta* **2019**, *191*, 81−88.

(11) Jiang, N.; Ahmed, R.; Damayantharan, M.; Ünal, B.; Butt, H.; Yetisen, A. K. Lateral and Vertical Flow Assays for Point-of-Care Diagnostics. *Adv. Healthc. Mater.* **2019**, *8* (14), No. 1900244.

(12) Joung, H. A.; Ballard, Z. S.; Ma, A.; Tseng, D. K.; Teshome, H.; Burakowski, S.; Garner, O. B.; Di Carlo, D.; Ozcan, A. Paper-based multiplexed vertical flow assay for point-of-care testing. *Lab Chip* **2019**, *19* (6), 1027−1034.
(13) Eryilmaz, M.; Goncharov, A.; Han, G.-R.; Joung, H.-A.; Ballard, Z. S.; Ghosh, R.; Zhang, Y.; Di Carlo, D.; Ozcan, A. A Paper-Based Multiplexed Serological Test to Monitor Immunity against SARS-COV-2 Using Machine Learning. *ACS Nano* **2024**, *18* (26), 16819−16831.
(14) Wang, J.; Mu, K.; Wei, H. J.; Chen, H.; Wang, Y. X.; Zhang, W. X.; Rong, Z. Paper-based multiplex colorimetric vertical flow assay with smartphone readout for point-of-care detection of acute kidney injury biomarkers. *Sens. Actuators B: Chem.* **2023**, *390*, No. 134029.
(15) Fu, X.; Xia, B.; Ji, B. C.; Lei, S.; Zhou, Y. Flow controllable three-dimensional paper-based microfluidic analytical devices fabricated by 3D printing technology. *Anal. Chim. Acta* **2019**, *1065*, 64−70.
(16) Liu, H.; Crooks, R. M. Three-Dimensional Paper Microfluidic Devices Assembled Using the Principles of Origami. *J. Am. Chem. Soc.* **2011**, *133* (44), 17564−17566.
(17) Scida, K.; Li, B.; Ellington, A. D.; Crooks, R. M. DNA detection using origami paper analytical devices. *Anal. Chem.* **2013**, *85* (20), 9713−9720.
(18) Park, C.; Kim, H. R.; Kim, S. K.; Jeong, I. K.; Pyun, J. C.; Park, S. Three-Dimensional Paper-Based Microfluidic Analytical Devices Integrated with a Plasma Separation Membrane for the Detection of Biomarkers in Whole Blood. *ACS Appl. Mater. Interfaces* **2019**, *11* (40), 36428−36434.
(19) Alba-Patiño, A.; Russell, S. M.; de la Rica, R. Origami-enabled signal amplification for paper-based colorimetric biosensors. *Sens. Actuators B: Chem.* **2018**, *273*, 951−954.
(20) Ballard, Z. S.; Joung, H. A.; Goncharov, A.; Liang, J. S.; Nugroho, K.; Di Carlo, D.; Garner, O. B.; Ozcan, A. Deep learning-enabled point-of-care sensing using multiplexed paper-based sensors. *NPJ. Digit. Med.* **2020**, *3* (1), 66.
(21) Goncharov, A.; Joung, H. A.; Ghosh, R.; Han, G. R.; Ballard, Z. S.; Maloney, Q.; Bell, A.; Aung, C. T. Z.; Garner, O. B.; Carlo, D. D.; et al. Deep Learning-Enabled Multiplexed Point-of-Care Sensor using a Paper-Based Fluorescence Vertical Flow Assay. *Small* **2023**, *19* (51), No. e2300617.
(22) Han, G. R.; Goncharov, A.; Eryilmaz, M.; Joung, H. A.; Ghosh, R.; Yim, G.; Chang, N.; Kim, M.; Ngo, K.; Veszpremi, M.; et al. Deep Learning-Enhanced Paper-Based Vertical Flow Assay for High-Sensitivity Troponin Detection Using Nanoparticle Amplification. *ACS Nano* **2024**, *18* (41), 27933−27948.
(23) Ghosh, R.; Joung, H. A.; Goncharov, A.; Palanisamy, B.; Ngo, K.; Pejcinovic, K.; Krockenberger, N.; Horn, E. J.; Garner, O. B.; Ghazal, E.; et al. Rapid single-tier serodiagnosis of Lyme disease. *Nat. Commun.* **2024**, *15* (1), 7124.
(24) Joung, H. A.; Ballard, Z. S.; Wu, J.; Tseng, D. K.; Teshome, H.; Zhang, L.; Horn, E. J.; Arnaboldi, P. M.; Dattwyler, R. J.; Garner, O. B.; et al. Point-of-Care Serodiagnostic Test for Early-Stage Lyme Disease Using a Multiplexed Paper-Based Immunoassay and Machine Learning. *ACS Nano* **2020**, *14* (1), 229−240.
(25) Ballard, Z.; Brown, C.; Madni, A. M.; Ozcan, A. Machine learning and computation-enabled intelligent sensor design. *Nat. Mach. Intell.* **2021**, *3* (7), 556−565.
(26) Koczula, K. M.; Gallotta, A. Lateral flow assays. *Essays Biochem.* **2016**, *60* (1), 111−120.
(27) Byrne, B.; Stack, E.; Gilmartin, N.; O'Kennedy, R. Antibody-Based Sensors: Principles, Problems and Potential for Detection of Pathogens and Associated Toxins. *Sensors* **2009**, *9* (6), 4407−4445.
(28) Wu, Y. H.; Zhou, Y. F.; Leng, Y. K.; Lai, W. H.; Huang, X. L.; Xiong, Y. H. Emerging design strategies for constructing multiplex lateral flow test strip sensors. *Biosens. Bioelectron.* **2020**, *157*, No. 112168.
(29) Ellington, A. A.; Kullo, I. J.; Bailey, K. R.; Klee, G. G. Antibody-Based Protein Multiplex Platforms: Technical and Operational Challenges. *Clin. Chem.* **2010**, *56* (2), 186−193.
(30) Juncker, D.; Bergeron, S.; Laforte, V.; Li, H. Y. Cross-reactivity in antibody microarrays and multiplexed sandwich assays: shedding light on the dark side of multiplexing. *Curr. Opin. Chem. Biol.* **2014**, *18*, 29−37.
(31) Sharma, S.; Zapatero-Rodriguez, J.; Estrela, P.; O'Kennedy, R. Point-of-Care Diagnostics in Low Resource Settings: Present Status and Future Role of Microfluidics. *Biosensors* **2015**, *5* (3), 577−601.
(32) Mak, W. C.; Beni, V.; Turner, A. P. F. Lateral-flow technology: From visual to instrumental. *TrAC, Trends Anal. Chem.* **2016**, *79*, 297−305.
(33) van den Berg, A.; Craighead, H. G.; Yang, P. From microfluidic applications to nanofluidic phenomena. *Chem. Soc. Rev.* **2010**, *39* (3), 899−900.
(34) Ben Aissa, A.; Araujo, B.; Julian, E.; Boldrin Zanoni, M. V.; Pividori, M. I. Immunomagnetic Separation Improves the Detection of Mycobacteria by Paper-Based Lateral and Vertical Flow Immunochromatographic Assays. *Sensors* **2021**, *21* (18), 5992.
(35) Martinez, A. W.; Phillips, S. T.; Butte, M. J.; Whitesides, G. M. Patterned paper as a platform for inexpensive, low-volume, portable bioassays. *Angew. Chem., Int. Ed.* **2007**, *46* (8), 1318−1320.
(36) Lei, R.; Wang, D.; Arain, H.; Mohan, C. Design of Gold Nanoparticle Vertical Flow Assays for Point-of-Care Testing. *Diagnostics* **2022**, *12* (5), 1107.
(37) Park, C.; Han, Y. D.; Kim, H. V.; Lee, J.; Yoon, H. C.; Park, S. Double-sided 3D printing on paper towards mass production of three-dimensional paper-based microfluidic analytical devices (3D-μPADs). *Lab Chip* **2018**, *18* (11), 1533−1538.
(38) Baek, S. H.; Park, C.; Jeon, J.; Park, S. Three-Dimensional Paper-Based Microfluidic Analysis Device for Simultaneous Detection of Multiple Biomarkers with a Smartphone. *Biosensors* **2020**, *10* (11), 187.
(39) Yong, T.; Kim, D.; Kim, S. Simultaneous multiple target detection platform based on vertical flow immunoassay. *J. Immunol. Methods* **2024**, *530*, No. 113690.
(40) Tahmasebi, M.; Bamdad, T.; Svendsen, W. E.; Forouzandeh-Moghadam, M. An enzymatic nucleic acid vertical flow assay. *Anal. Bioanal. Chem.* **2022**, *414* (12), 3605−3615.
(41) Ge, L.; Wang, S. M.; Song, X. R.; Ge, S. G.; Yu, J. H. 3D Origami-based multifunction-integrated immunodevice: low-cost and multiplexed sandwich chemiluminescence immunoassay on microfluidic paper-based analytical device. *Lab Chip* **2012**, *12* (17), 3150−3158.
(42) Park, J.; Park, J. K. Pressed region integrated 3D paper-based microfluidic device that enables vertical flow multistep assays for the detection of C-reactive protein based on programmed reagent loading. *Sens. Actuators B: Chem.* **2017**, *246*, 1049−1055.
(43) Chin, C. D.; Linder, V.; Sia, S. K. Commercialization of microfluidic point-of-care diagnostic devices. *Lab Chip* **2012**, *12* (12), 2118−2134.
(44) Budd, J.; Miller, B. S.; Weckman, N. E.; Cherkaoui, D.; Huang, D.; Decruz, A. T.; Fongwen, N.; Han, G.-R.; Broto, M.; Estcourt, C. S.; et al. Lateral flow test engineering and lessons learned from COVID-19. *Nat. Rev. Bioeng.* **2023**, *1* (1), 13−31.
(45) Nadar, S. S.; Patil, P. D.; Tiwari, M. S.; Ahirrao, D. J. Enzyme embedded microfluidic paper-based analytic device (μPAD): a comprehensive review. *Crit. Rev. Biotechnol.* **2021**, *41* (7), 1046−1080.
(46) Tay, D. M. Y.; Kim, S.; Hao, Y. N.; Yee, E. H.; Jia, H.; Vleck, S. M.; Chilekwa, M.; Voldman, J.; Sikes, H. D. Accelerating the optimization of vertical flow assay performance guided by a rational systematic model-based approach. *Biosens. Bioelectron.* **2023**, *222*, No. 114977.
(47) Boumar, I.; Deliorman, M.; Sukumar, P.; Qasaimeh, M. A. Spike- and nucleocapsid-based gold colloid assay toward the development of an adhesive bandage for rapid SARS-CoV-2 immune response detection and screening. *Microsyst. Nanoeng.* **2023**, *9* (1), 82.
(48) Chen, C. A.; Yeh, W. S.; Tsai, T. T.; Li, Y. D.; Chen, C. F. Three-dimensional origami paper-based device for portable immunoassay applications. *Lab Chip* **2019**, *19* (4), 598−607.

https://doi.org/10.1021/acssensors.5c00668
ACS Sens. 2025, 10, 3317−3339

(49) Noh, N.; Phillips, S. T. Metering the Capillary-Driven Flow of Fluids in Paper-Based Microfluidic Devices. *Anal. Chem.* **2010**, *82* (10), 4181−4187.
(50) Toda, H.; Iwasaki, W.; Morita, N.; Motomura, T.; Takemura, K.; Nagano, M.; Nakanishi, Y.; Nakashima, Y. Reversible Thermo-Responsive Valve for Microfluidic Paper-Based Analytical Devices. *Micromachines* **2022**, *13* (5), 690.
(51) Then, W. L.; Garnier, G. Paper diagnostics in biomedicine. *Rev. Anal. Chem.* **2013**, *32* (4), 269−294.
(52) Kakkar, S.; Gupta, P.; Singh Yadav, S. P.; Raj, D.; Singh, G.; Chauhan, S.; Mishra, M. K.; Martin-Ortega, E.; Chiussi, S.; Kant, K. Lateral flow assays: Progress and evolution of recent trends in point-of-care applications. *Mater. Today Bio* **2024**, *28*, No. 101188.
(53) Sajid, M.; Kawde, A.-N.; Daud, M. Designs, formats and applications of lateral flow assay: A literature review. *J. Saudi Chem. Soc.* **2015**, *19* (6), 689−705.
(54) Kasetsirikul, S.; Shiddiky, M. J. A.; Nguyen, N.-T. Challenges and perspectives in the development of paper-based lateral flow assays. *Microfluid. Nanofluidics* **2020**, *24* (2), 17.
(55) O'Farrell, B. Lateral Flow Technology for Field-Based Applications—Basics and Advanced Developments. *Top. Companion Anim. Med.* **2015**, *30* (4), 139−147.
(56) Serhan, M.; Jackemeyer, D.; Abi Karam, K.; Chakravadhanula, K.; Sprowls, M.; Cay-Durgun, P.; Forzani, E. A novel vertical flow assay for point of care measurement of iron from whole blood. *Analyst* **2021**, *146* (5), 1633−1641.
(57) Pollock, N. R.; McGray, S.; Colby, D. J.; Noubary, F.; Nguyen, H.; Nguyen, T. A.; Khormaee, S.; Jain, S.; Hawkins, K.; Kumar, S.; et al. Field evaluation of a prototype paper-based point-of-care fingerstick transaminase test. *PLoS One* **2013**, *8* (9), No. e75616.
(58) Jin, J. H.; Kim, J. H.; Lee, S. K.; Choi, S. J.; Park, C. W.; Min, N. K. A Fully Integrated Paper-Microfluidic Electrochemical Device for Simultaneous Analysis of Physiologic Blood Ions. *Sensors* **2018**, *18* (1), 104.
(59) Li, W.; Qian, D.; Wang, Q.; Li, Y.; Bao, N.; Gu, H.; Yu, C. Fully-drawn origami paper analytical device for electrochemical detection of glucose. *Sens. Actuators B: Chem.* **2016**, *231*, 230−238.
(60) Li, M.; Wang, L.; Liu, R.; Li, J.; Zhang, Q.; Shi, G.; Li, Y.; Hou, C.; Wang, H. A highly integrated sensing paper for wearable electrochemical sweat analysis. *Biosens. Bioelectron* **2021**, *174*, No. 112828.
(61) Li, X.; Luo, L.; Crooks, R. M. Low-voltage paper isotachophoresis device for DNA focusing. *Lab Chip* **2015**, *15* (20), 4090−4098.
(62) Jiao, Y.; Du, C.; Zong, L.; Guo, X.; Han, Y.; Zhang, X.; Li, L.; Zhang, C.; Ju, Q.; Liu, J.; et al. 3D vertical-flow paper-based device for simultaneous detection of multiple cancer biomarkers by fluorescent immunoassay. *Sens. Actuators B: Chem.* **2020**, *306*, No. 127239.
(63) Connelly, J. T.; Rolland, J. P.; Whitesides, G. M. "Paper Machine" for Molecular Diagnostics. *Anal. Chem.* **2015**, *87* (15), 7595−7601.
(64) Lei, R.; Arain, H.; Wang, D.; Arunachalam, J.; Saxena, R.; Mohan, C. Duplex Vertical-Flow Rapid Tests for Point-of-Care Detection of Anti-dsDNA and Anti-Nuclear Autoantibodies. *Biosensors* **2024**, *14* (2), 98.
(65) Prajapati, A.; Verma, N.; Pandya, A. Highly sensitive vertical flow based point-of-care immunokit for rapid and early detection of human CRP as a cardiovascular risk factor. *Biomed. Microdevices* **2020**, *22* (2), 28.
(66) Kropaneva, M.; Khramtsov, P.; Bochkova, M.; Lazarev, S.; Kiselkov, D.; Rayev, M. Vertical Flow Immunoassay Based on Carbon Black Nanoparticles for the Detection of IgG against SARS-CoV-2 Spike Protein in Human Serum: Proof-of-Concept. *Biosensors* **2023**, *13* (9), 857.
(67) Yang, Z.; Xu, G.; Reboud, J.; Ali, S. A.; Kaur, G.; McGiven, J.; Boby, N.; Gupta, P. K.; Chaudhuri, P.; Cooper, J. M. Rapid Veterinary Diagnosis of Bovine Reproductive Infectious Diseases from Semen Using Paper-Origami DNA Microfluidics. *ACS Sens.* **2018**, *3* (2), 403−409.
(68) Xu, G.; Nolder, D.; Reboud, J.; Oguike, M. C.; van Schalkwyk, D. A.; Sutherland, C. J.; Cooper, J. M. Paper-Origami-Based Multiplexed Malaria Diagnostics from Whole Blood. *Angew. Chem., Int. Ed.* **2016**, *55* (49), 15250−15253.
(69) Biswas, P.; Mukunthan Sulochana, G. N.; Banuprasad, T. N.; Goyal, P.; Modak, D.; Ghosh, A. K.; Chakraborty, S. All-Serotype Dengue Virus Detection through Multilayered Origami-Based Paper/Polymer Microfluidics. *ACS Sens.* **2022**, *7* (12), 3720−3729.
(70) Sun, Y.; Chang, Y.; Zhang, Q.; Liu, M. An Origami Paper-Based Device Printed with DNAzyme-Containing DNA Superstructures for Escherichia coli Detection. *Micromachines* **2019**, *10* (8), 531.
(71) Lei, R.; Arain, H.; Obaid, M.; Sabhnani, N.; Mohan, C. Ultra-Sensitive and Semi-Quantitative Vertical Flow Assay for the Rapid Detection of Interleukin-6 in Inflammatory Diseases. *Biosensors* **2022**, *12* (9), 756.
(72) Kaur, M.; Eltzov, E. Optimizing Effective Parameters to Enhance the Sensitivity of Vertical Flow Assay for Detection of Escherichia coli. *Biosensors* **2022**, *12* (2), 63.
(73) Kim, S.; Hao, Y.; Miller, E. A.; Tay, D. M. Y.; Yee, E.; Kongsuphol, P.; Jia, H.; McBee, M.; Preiser, P. R.; Sikes, H. D. Vertical Flow Cellulose-Based Assays for SARS-CoV-2 Antibody Detection in Human Serum. *ACS Sens.* **2021**, *6* (5), 1891−1898.
(74) Jia, H.; Miller, E. A.; Chan, C. C.; Ng, S. Y.; Prabakaran, M.; Tao, M.; Cheong, I. S.; Lim, S. M.; Chen, M. W.; Gao, X.; et al. Development and translation of a paper-based top readout vertical flow assay for SARS-CoV-2 surveillance. *Lab Chip* **2022**, *22* (7), 1321−1332.
(75) Vaquer, A.; Adrover-Jaume, C.; Clemente, A.; Viana, J.; Rodríguez, R.; Rojo-Molinero, E.; Oliver, A.; de la Rica, R. OriPlex: Origami-enabled multiplexed detection of respiratory pathogens. *Biosens. and Bioelectron.* **2024**, *257*, No. 116341.
(76) Biswas, P.; Mukherjee, A.; Goyal, P.; Bhattacharya, P.; Dutta, G.; Chakraborty, S. A rapid diagnostic technology for isolating rare blood group patients under medical emergency using a three-fold paper-polymer microfluidic kit. *Sens. Actuators B: Chem.* **2024**, *409*, No. 135650.
(77) Ye, D.; Li, L.; Li, Z.; Zhang, Y.; Li, M.; Shi, J.; Wang, L.; Fan, C.; Yu, J.; Zuo, X. Molecular Threading-Dependent Mass Transport in Paper Origami for Single-Step Electrochemical DNA Sensors. *Nano Lett.* **2019**, *19* (1), 369−374.
(78) Luo, L.; Li, X.; Crooks, R. M. Low-voltage origami-paper-based electrophoretic device for rapid protein separation. *Anal. Chem.* **2014**, *86* (24), 12390−12397.
(79) Cheng, H. L.; Jia, H.; Lim, S. M.; Ng, S. Y.; Kongsuphol, P.; McBee, M. E.; Sikes, H. D. Development of a cellulose-based 96-well plate vertical flow pull-down assay. *Anal. Methods* **2023**, *15* (28), 3483−3489.
(80) Suvanasuthi, R.; Chimnaronk, S.; Promptmas, C. 3D printed hydrophobic barriers in a paper-based biosensor for point-of-care detection of dengue virus serotypes. *Talanta* **2022**, *237*, No. 122962.
(81) Morbioli, G. G.; Mazzu-Nascimento, T.; Milan, L. A.; Stockton, A. M.; Carrilho, E. Improving Sample Distribution Homogeneity in Three-Dimensional Microfluidic Paper-Based Analytical Devices by Rational Device Design. *Anal. Chem.* **2017**, *89* (9), 4786−4792.
(82) Sun, K.; Fan, Y.; Hebda, M.; Zhang, Y. Origami Microfluidics: A Review of Research Progress and Biomedical Applications. *Biomed. Mater. Devices* **2023**, *1* (1), 388−401.
(83) Govindarajan, A. V.; Ramachandran, S.; Vigil, G. D.; Yager, P.; Bohringer, K. F. A low cost point-of-care viscous sample preparation device for molecular diagnosis in the developing world; an example of microfluidic origami. *Lab Chip* **2012**, *12* (1), 174−181.
(84) Jeon, J.; Park, C.; Ponnuvelu, D. V.; Park, S. Enhanced Sensing Behavior of Three-Dimensional Microfluidic Paper-Based Analytical Devices (3D-μPADs) with Evaporation-Free Enclosed Channels for Point-of-Care Testing. *Diagnostics* **2021**, *11* (6), 977.
(85) Xue, W.; Zhao, D.; Zhang, Q.; Chang, Y. Y.; Liu, M. An origami paper-based analytical device for DNA damage analysis. *Chem. Commun.* **2021**, *57* (87), 11465−11468.

https://doi.org/10.1021/acssensors.5c00668
ACS Sens. 2025, 10, 3317−3339

(86) Sheini, A. A paper-based device for the colorimetric determination of ammonia and carbon dioxide using thiomalic acid and maltol functionalized silver nanoparticles: application to the enzymatic determination of urea in saliva and blood. *Microchim. Acta* **2020**, *187* (10), 565.
(87) Ding, J.; Li, B.; Chen, L.; Qin, W. A Three-Dimensional Origami Paper-Based Device for Potentiometric Biosensing. *Angew. Chem., Int. Ed. Engl.* **2016**, *55* (42), 13033−13037.
(88) Sheini, A.; Aseman, M. D.; Bordbar, M. M. Origami paper analytical assay based on metal complex sensor for rapid determination of blood cyanide concentration in fire survivors. *Sci. Rep.* **2021**, *11* (1), 3521.
(89) Shen, Y.; Modha, S.; Tsutsui, H.; Mulchandani, A. An origami electrical biosensor for multiplexed analyte detection in body fluids. *Biosens. Bioelectron.* **2021**, *171*, No. 112721.
(90) Kalligosfyri, P. M.; Cinti, S. 3D Paper-Based Origami Device for Programmable Multifold Analyte Preconcentration. *Anal. Chem.* **2024**, *96* (24), 9773−9779.
(91) Zhang, T.; Deng, R.; Wang, Y.; Wu, C.; Zhang, K.; Wang, C.; Gong, N.; Ledesma-Amaro, R.; Teng, X.; Yang, C.; et al. A paper-based assay for the colorimetric detection of SARS-CoV-2 variants at single-nucleotide resolution. *Nat. Biomed. Eng.* **2022**, *6* (8), 957−967.
(92) Trieu, P. T.; Lee, N. Y. Paper-Based All-in-One Origami Microdevice for Nucleic Acid Amplification Testing for Rapid Colorimetric Identification of Live Cells for Point-of-Care Testing. *Anal. Chem.* **2019**, *91* (17), 11013−11022.
(93) Lewis, G. G.; Robbins, J. S.; Phillips, S. T. Point-of-Care Assay Platform for Quantifying Active Enzymes to Femtomolar Levels Using Measurements of Time as the Readout. *Anal. Chem.* **2013**, *85* (21), 10432−10439.
(94) Verma, M. S.; Tsaloglou, M. N.; Sisley, T.; Christodouleas, D.; Chen, A.; Milette, J.; Whitesides, G. M. Sliding-strip microfluidic device enables ELISA on paper. *Biosens. Bioelectron.* **2018**, *99*, 77−84.
(95) Renault, C.; Li, X.; Fosdick, S. E.; Crooks, R. M. Hollow-channel paper analytical devices. *Anal. Chem.* **2013**, *85* (16), 7976−7979.
(96) Im, S. H.; Kim, K. R.; Park, Y. M.; Yoon, J. H.; Hong, J. W.; Yoon, H. C. An animal cell culture monitoring system using a smartphone-mountable paper-based analytical device. *Sens. Actuators B: Chem.* **2016**, *229*, 166−173.
(97) Bhardwaj, J.; Sharma, A.; Jang, J. Vertical flow-based paper immunosensor for rapid electrochemical and colorimetric detection of influenza virus using a different pore size sample pad. *Biosens. Bioelectron.* **2019**, *126*, 36−43.
(98) Han, K. N.; Choi, J. S.; Kwon, J. Three-dimensional paper-based slip device for one-step point-of-care testing. *Sci. Rep.* **2016**, *6*, No. 25710.
(99) Faizul Zaki, M.; Chen, P.-C.; Yeh, Y.-C.; Lin, P.-H.; Xu, M.-Y. Engineering a monolithic 3D paper-based analytical device (μPAD) by stereolithography 3D printing and sequential digital masks for efficient 3D mixing and dopamine detection. *Sens. Actuators A: Phys.* **2022**, *347*, No. 113991.
(100) Han, G. R.; Goncharov, A.; Eryilmaz, M.; Ye, S.; Joung, H. A.; Ghosh, R.; Ngo, E.; Tomoeda, A.; Lee, Y.; Ngo, K. Deep learning-enhanced chemiluminescence vertical flow assay for high-sensitivity cardiac troponin I testing. *arXiv*, 2412.08945, 2024. DOI: 10.48550/arXiv.2412.08945.
(101) Weber, L. K.; Palermo, A.; Kügler, J.; Armant, O.; Isse, A.; Rentschler, S.; Jaenisch, T.; Hubbuch, J.; Dübel, S.; Nesterov-Mueller, A.; et al. Single amino acid fingerprinting of the human antibody repertoire with high density peptide arrays. *J. Immunol. Methods* **2017**, *443*, 45−54.
(102) Heiss, K.; Heidepriem, J.; Fischer, N.; Weber, L. K.; Dahlke, C.; Jaenisch, T.; Loeffler, F. F. Rapid Response to Pandemic Threats: Immunogenic Epitope Detection of Pandemic Pathogens for Diagnostics and Vaccine Development Using Peptide Microarrays. *J. Proteome Res.* **2020**, *19* (11), 4339−4354.
(103) Sharifi, H.; Tashkhourian, J.; Hemmateenejad, B. A 3D origami paper-based analytical device combined with PVC membrane for colorimetric assay of heavy metal ions: Application to determination of Cu(II) in water samples. *Anal. Chim. Acta* **2020**, *1126*, 114−123.
(104) Choi, J.; Lee, E. H.; Kang, S. M.; Jeong, H. H. A Facile Method to Fabricate an Enclosed Paper-Based Analytical Device via Double-Sided Patterning for Ionic Contaminant Detection. *Biosensors* **2023**, *13* (10), 915.
(105) Colozza, N.; Tazzioli, S.; Sassolini, A.; Agosta, L.; di Monte, M. G.; Hermansson, K.; Arduini, F. Vertical-Flow Paper Sensor for On-Site and Prompt Evaluation of Chloride Contamination in Concrete Structures. *Anal. Chem.* **2021**, *93* (43), 14369−14374.
(106) Martínez-Pérez-Cejuela, H.; Mesquita, R. B. R.; Simó-Alfonso, E. F.; Herrero-Martínez, J. M.; Rangel, A. O. S. S. Combining microfluidic paper-based platform and metal-organic frameworks in a single device for phenolic content assessment in fruits. *Microchim. Acta* **2023**, *190* (4), 126.
(107) Martínez-Pérez-Cejuela, H.; Mesquita, R. B. R.; Couto, J. A.; Simó-Alfonso, E. F.; Herrero-Martínez, J. M.; Rangel, A. O. S. S. Design of a microfluidic paper-based device for the quantification of phenolic compounds in wine samples. *Talanta* **2022**, *250*, No. 123747.
(108) Nogueira, S. A.; Lemes, A. D.; Chagas, A. C.; Vieira, M. L.; Talhavini, M.; Morais, P. A. O.; Coltro, W. K. T. Redox titration on foldable paper-based analytical devices for the visual determination of alcohol content in whiskey samples. *Talanta* **2019**, *194*, 363−369.
(109) Custodio-Mendoza, J. A.; Pokorski, P.; Aktas, H.; Napiorkowska, A.; Kurek, M. A. Advances in Chromatographic Analysis of Phenolic Phytochemicals in Foods: Bridging Gaps and Exploring New Horizons. *Foods* **2024**, *13* (14), 2268.
(110) Chaiyo, S.; Apiluk, A.; Siangproh, W.; Chailapakul, O. High sensitivity and specificity simultaneous determination of lead, cadmium and copper using μPAD with dual electrochemical and colorimetric detection. *Sens. Actuators B: Chem.* **2016**, *233*, 540−549.
(111) Jang, I.; Carrão, D. B.; Menger, R. F.; Moraes de Oliveira, A. R.; Henry, C. S. Pump-Free Microfluidic Rapid Mixer Combined with a Paper-Based Channel. *ACS Sens.* **2020**, *5* (7), 2230−2238.
(112) Nashukha, H. L.; Sitanurak, J.; Sulistyarti, H.; Nacapricha, D.; Uraisin, K. Simple and Equipment-Free Paper-Based Device for Determination of Mercury in Contaminated Soil. *Molecules* **2021**, *26* (7), 2004.
(113) Li, F.; Hu, Y.; Li, Z.; Liu, J.; Guo, L.; He, J. Three-dimensional microfluidic paper-based device for multiplexed colorimetric detection of six metal ions combined with use of a smartphone. *Anal. Bioanal. Chem.* **2019**, *411* (24), 6497−6508.
(114) Zhou, J.; Li, B.; Qi, A.; Shi, Y.; Qi, J.; Xu, H.; Chen, L. ZnSe quantum dot based ion imprinting technology for fluorescence detecting cadmium and lead ions on a three-dimensional rotary paper-based microfluidic chip. *Sens. Actuators B: Chem.* **2020**, *305*, No. 127462.
(115) Wang, M.; Song, Z.; Jiang, Y.; Zhang, X.; Wang, L.; Zhao, H.; Cui, Y.; Gu, F.; Wang, Y.; Zheng, G. A three-dimensional pinwheel-shaped paper-based microfluidic analytical device for fluorescence detection of multiple heavy metals in coastal waters by rational device design. *Anal. Bioanal. Chem.* **2021**, *413* (12), 3299−3313.
(116) Kim, H. J.; Kim, Y.; Park, S. J.; Kwon, C.; Noh, H. Development of Colorimetric Paper Sensor for Pesticide Detection Using Competitive-inhibiting Reaction. *BioChip J.* **2018**, *12* (4), 326−331.
(117) Lin, J.-H.; Chen, S.-J.; Lee, J.-E.; Chu, W.-Y.; Yu, C.-J.; Chang, C.-C.; Chen, C.-F. The detection of Mercury(II) ions using fluorescent gold nanoclusters on a portable paper-based device. *Chem. Eng. J.* **2022**, *430*, No. 133070.
(118) Wu, H.; Chen, J.; Yang, Y.; Yu, W.; Chen, Y.; Lin, P.; Liang, K. Smartphone-coupled three-layered paper-based microfluidic chips demonstrating stereoscopic capillary-driven fluid transport towards colorimetric detection of pesticides. *Anal. Bioanal. Chem.* **2022**, *414* (5), 1759−1772.

(119) Sun, H.; Jia, Y.; Dong, H.; Fan, L. Graphene oxide nanosheets coupled with paper microfluidics for enhanced on-site airborne trace metal detection. *Microsyst. Nanoeng.* **2019**, *5* (1), 4.
(120) Arduini, F.; Cinti, S.; Caratelli, V.; Amendola, L.; Palleschi, G.; Moscone, D. Origami multiple paper-based electrochemical biosensors for pesticide detection. *Biosens. Bioelectron.* **2019**, *126*, 346−354.
(121) Placer, L.; Lavilla, I.; Pena-Pereira, F.; Bendicho, C. A 3D microfluidic paper-based analytical device with smartphone-assisted colorimetric detection for iodine speciation in seaweed samples. *Sens. Actuators B: Chem.* **2023**, *377*, No. 133109.
(122) Aryal, P.; Brack, E.; Alexander, T.; Henry, C. S. Capillary Flow-Driven Microfluidics Combined with a Paper Device for Fast User-Friendly Detection of Heavy Metals in Water. *Anal. Chem.* **2023**, *95* (13), 5820−5827.
(123) Lee, S.; Park, J.; Park, J.-K. Foldable paper-based analytical device for the detection of an acetylcholinesterase inhibitor using an angle-based readout. *Sens. Actuators B: Chem.* **2018**, *273*, 322−327.
(124) Chen, R.; Liu, B.; Ni, H.; Chang, N.; Luan, C.; Ge, Q.; Dong, J.; Zhao, X. Vertical flow assays based on core−shell SERS nanotags for multiplex prostate cancer biomarker detection. *Analyst* **2019**, *144* (13), 4051−4059.
(125) Jang, H.-J.; Joung, H.-A.; Goncharov, A.; Kanegusuku, A. G.; Chan, C. W.; Yeo, K.-T. J.; Zhuang, W.; Ozcan, A.; Chen, J. Deep Learning-Based Kinetic Analysis in Paper-Based Analytical Cartridges Integrated with Field-Effect Transistors. *ACS Nano* **2024**, *18* (36), 24792−24802.
(126) Misra, S.; Huddy, J.; Hanna, G.; Oliver, N. Validation and regulation of point of care devices for medical applications. *Medical Biosensors for Point of Care (POC) Applications* **2017**, 27−44.
(127) Han, G.-R.; Goncharov, A.; Eryilmaz, M.; Ye, S.; Palanisamy, B.; Ghosh, R.; Lisi, F.; Rogers, E.; Guzman, D.; Yigci, D.; et al. Machine learning in point-of-care testing: innovations, challenges, and opportunities. *Nat. Commun.* **2025**, *16* (1), 3165.
(128) Wang, B.; Li, Y.; Zhou, M.; Han, Y.; Zhang, M.; Gao, Z.; Liu, Z.; Chen, P.; Du, W.; Zhang, X.; et al. Smartphone-based platforms implementing microfluidic detection with image-based artificial intelligence. *Nat. Commun.* **2023**, *14* (1), 1341.
(129) Cui, F.; Yue, Y.; Zhang, Y.; Zhang, Z.; Zhou, H. S. Advancing Biosensors with Machine Learning. *ACS Sens.* **2020**, *5* (11), 3346−3364.
(130) Bhaiyya, M.; Panigrahi, D.; Rewatkar, P.; Haick, H. Role of Machine Learning Assisted Biosensors in Point-of-Care-Testing For Clinical Decisions. *ACS Sens.* **2024**, *9* (9), 4495−4519.
(131) Han, G.-R.; Koo, H. J.; Ki, H.; Kim, M.-G. Paper/Soluble Polymer Hybrid-Based Lateral Flow Biosensing Platform for High-Performance Point-of-Care Testing. *ACS Appl. Mater. Interfaces* **2020**, *12* (31), 34564−34575.
(132) Han, G.-R.; Ki, H.; Kim, M.-G. Automated, Universal, and Mass-Producible Paper-Based Lateral Flow Biosensing Platform for High-Performance Point-of-Care Testing. *ACS Appl. Mater. Interfaces* **2020**, *12* (1), 1885−1894.

https://doi.org/10.1021/acssensors.5c00668
ACS Sens. 2025, 10, 3317−3339